ELSEVIER

Journal of Nuclear Materials 246 (1997) 91–120

journal of nuclear materials

Review

Assessment of relative contributions from different mechanisms to radiation embrittlement of reactor pressure vessel steels

B.A. Gurovich *, E.A. Kuleshova, Yu.A. Nikolaev, Ya.I. Shtrombakh

Russian Research Center, Kurchatov Institute, Kurchatov sq.1, Moscow 123182, Russia

Received 24 October 1996; accepted 9 April 1997

Abstract

Experimental data on radiation embrittlement in pressure vessel steels of both Russian and American grades, obtained by the authors and also taken from the literature, have been analyzed to assess the relative contributions from the following mechanisms: radiation-induced hardening, inter- and intragranular segregation of impurities at precipitate/matrix interfaces. It is demonstrated that radiation-induced intragranular segregation of impurities frequently provides a significant contribution to radiation embrittlement of pressure vessel steels. © 1997 Elsevier Science B.V.

1. Introduction

A key problem in nuclear material science is the elucidation of the nature of radiation embrittlement (RE) of pressure vessel materials in a pressurized water reactor (PWR) resulting from irradiation. Studies carried out in the last few decades in several countries have shown that the irradiation environment experienced by the reactor pressure vessel of a thermal reactor can produce significant RE of steels used in the construction of such vessels [1]. First and foremost, the effect of irradiation manifests itself as an appreciable upward shift in ductile-to-brittle transition temperature (DBTT) as observed in the Charpy energy transition curve (the temperature dependence of absorbed energy) [1]. This shift makes brittle fracture of the reactor pressure vessel more probable in certain situations during operation. Precautions that are usually taken to ensure the safety of nuclear reactors of the PWR type are designated to preclude the possibility of brittle fracture of the pressure vessel under various maximum emergency scenarios.

The rate and degree of RE in reactor pressure vessel steels (RPVS) can limit PWR lifetime and thus define the safety and profitability of their operation. To extend the operating lifetime, a few 'old' pressure vessels made from materials with high rates of RE have undergone recovery annealing [2]. Therefore, the nature and mechanisms of RE, as well as changes in properties of the materials after post-irradiation annealing and re-irradiation, are the subjects of major studies.

2. Background to radiation embrittlement problem

Although a considerable number of publications associated with the problem of RE in RPVS have been presented in the last few decades [1–6], an adequate understanding of the nature of the phenomenon is still not complete. The reason is the complexity and diversity of the processes thought to occur in irradiated steels. The available experimental data show that irradiation of RPVS under conditions characteristic of a PWR (irradiation temperature of ~ 240–290°C, fast neutron fluence $< 2 \times 10^{24}$ n m^{-2}, the period of irradiation at the temperature being decades) might induce the following specific changes in material microstructure:

(i) Formation of radiation defects [4,7,8].

(ii) Phase transformations accompanied by the generation of various precipitate populations [9].

(iii) Formation of impurity-vacancy clusters (for instance, copper-vacancy ones) [4,8,97].

* Corresponding author.

0022-3115/97/$17.00 © 1997 Elsevier Science B.V. All rights reserved.
PII S0022-3115(97)00103-7

(iv) Segregation of phosphorus and probably some other impurities [10–12] to grain boundaries (i.e., intergranular segregation).

(v) Impurity segregation (e.g., phosphorus) to interfaces between secondary phases and matrix and/or radiation defects [13] (i.e., intragranular segregation).

The above radiation-induced structural changes may induce complex, synergistic changes in steel behaviour, which cannot be explained with the use of a single mechanism. Noteworthy is that a satisfactory predictive description, based on fundamental principles, of any of the above mentioned radiation-induced phenomena is essentially unattainable at present. For example, to obtain a predictive description of the kinetics of accumulation of radiation defects, it is necessary to know parameters such as the recombination efficiency of point defects, details of atomic collision cascades, preferential characteristics of various sink types, the influence of impurities and alloying elements on the latter and many other material characteristics. To describe the influence of radiation defects and precipitate populations on material hardening, it is necessary to know their individual strengths as barriers for dislocations and certain other parameters. Such data are only partially available even for simple alloys, whilst the situation is even less favourable for complex alloys such as RPVS. Therefore a phenomenological description of any of the processes mentioned above necessarily requires the introduction of a large number of fitting parameters [3,14–16]. For this reason it is difficult to quantify the degree of applicability and validity of these models. Nevertheless, they are necessary for the development of notions and concepts in the study of embrittlement.

The specific difficulty in the theoretical description of the phenomenon of RE in pressure vessel materials is that the value of the DBTT shift (ΔTT) [17–19] used in practical engineering problems cannot be readily defined as a physical value. There are two reasons for this situation.

(1) The reference levels applied for the numerical determination of the DBTT from the curve of absorbed energy versus temperature cannot be obtained from physical considerations. Worldwide a range of values of absorbed energy is used for this purpose: 28, 30, 41, 47, 60 and 70 J, for example.

(2) The transition curve (temperature dependence of absorbed energy) for Charpy specimens (in impact testing) after irradiation is shifted non-equidistantly upwards (Fig. 1). This effect is caused by a change in the slope of the curve in the transition region resulting from irradiation and also by a decrease in the level of the upper shelf energy (USE) (Fig. 1).

These difficulties do not permit a proper theoretical model of RE based on ab initio principles to be developed. In particular, it is impossible to develop proper models associating the value of ΔTT with physical properties of steels, for example, with yield stress. Such models can be developed for another well known phenomenon, namely, the radiation swelling in stainless steels.

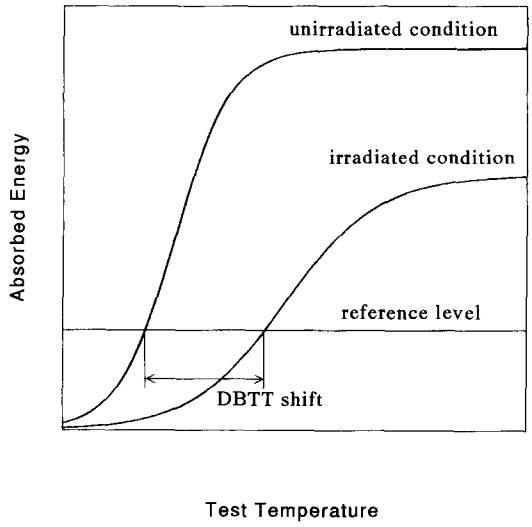

Fig. 1. Schematic showing the influence of irradiation on DBTT curve.

Thus, all available relationships between the value of ΔTT and various properties, structural parameters of steels, their composition, irradiation and recovery annealing conditions can be only empirical ones for the reasons noted above. For the same reason, experimental studies dominate the investigation of the nature and mechanisms defining RE in RPVS.

It is well known that the most widely used RPVS can be conventionally divided into several classes as follows:

(i) Steels of American grades characterized by a low content of chromium (typically ~0.1–0.14%), low (typically ~0.18% in A302) or increased (typically ~0.62 (0.40–0.70, specification) and ~0.75 (0.40–1.00, specification) in A533 and A508, respectively) content of nickel.

(ii) Russian types of steels with an increased content of chromium (2–3%), low (< 0.4 (typically ~0.2%) in 15Kh2MFA) and increased (1–2% in 15Kh2NMFA) content of nickel.

Empirical relationships between fast neutron fluence and chemical composition of steels and the degree of RE have been revealed from processing a large body of experimental data on RPVS. Usually these relations have the form

$$\Delta TT = A \times F^n, \tag{1}$$

where A is a parameter depending on the chemical composition of the steel, n is the exponent and F the fast neutron fluence. In the US NRC Regulatory Guide 1.99, Rev.1 [17] the following relationships are given:

$$\Delta TT = 3/5\left[40 + 1000(C_{Cu} - 0.08) + 5000(C_P - 0.008)\right]F^{1/2}, \tag{2}$$

where C_i (i = Cu or P) represents the element concentration in wt%, F is the neutron fluence in terms of 10^{23} n m^{-2} ($E < 1$ MeV), if the real content of Cu does not exceed 0.08%, then $C_{Cu} = 0.08\%$ and if the real content of P does not exceed 0.008%, then $C_P = 0.008\%$. The US NRC Regulatory Guide 1.99, Rev.2 [18] gives the following expression for the trend curve of A302B, A508 and A533B steels:

$$\Delta TT = 3/5(CF)F^{(0.28-0.10\log F)}\ (^\circ C), \tag{3}$$

where CF (°F) is a chemical factor given in terms of Cu and Ni content and tabulated in Ref. [18].

The equivalent in Russian standards [19] is given by

$$\Delta TT = 800(C_P + 0.07C_{Cu})F^{1/3}, \tag{4}$$

where F is the fluence in terms of 10^{22} n m^{-2} ($E > 0.5$ MeV).

Analysis of Eqs. (2)–(4) has shown that copper is the most significant impurity in American steels. In the US NRC Regulatory Guide 1.99, Rev.2 [18], the influence of phosphorus on RE is not taken into account at all. However, in Russian WWER-440 steels the concentration of phosphorus is the most significant factor. The empirical character of Eqs. (2)–(4) severely restricts the area of their reliable application in terms of experimental conditions (irradiation temperatures, fluences and fluxes of fast neutrons, concentrations of alloy and impurity elements, etc.).

It is also worth noting that the number of experiments aimed at investigating the effect of alloy and impurity concentrations in steels on the degree of RE is relatively few. Moreover, in such experimental studies the known mathematical algorithms [20] allowing a correct estimation of contributions from one or another elements or their combinations to changes of some properties, for instance, to RE, were not applied.

The major portion of data on RE was obtained for RPVS with random commercial contents of impurities and alloying elements [3,5,15]. Moreover, the situation is made more difficult since a synergism exists between the characteristics of the alloy and the impurity influence on the value of RE in the steels (ΔTT) and, furthermore, the value of ΔTT depends non-linearly on irradiation temperature [1,21], fluence [1,17–19] and, probably, neutron flux [22,23].

Thus, one cannot exclude that probably the determinative influence of some alloying elements and/or impurities, or their combinations, which inevitably exist in the steels as an interfering factor, on parameter A in Eq. (1), has not been taken into account in Eqs. (2)–(4). This factor depends on the properties of the raw materials and details of the metallurgical process. Similar examples are known in material science. For instance, it was shown in studies of temperature dependence of yield stress that in pure α-Fe with a carbon content < 0.005 ppm, this dependence becomes reduced [24]. Carbon does not effect RE for concentrations typical of the steels. Similar examples can be drawn from researches on irradiated materials. Numerous works devoted to swelling occurring in austenitic stainless steels in irradiation conditions characteristic of fast-neutron reactors show that the degree and rate of swelling in the transient stage depend on neutron fluence, chemical and phase content of the steels, density of dislocations, presence of boron (and its isotopic content), etc. [25]. However, in the steady-state stage of swelling, the rate becomes practically a structurally-independent value [25]. But this is commonly accepted at the present time that if gas impurities are absent, then no swelling in steels occurs, because 3D vacancy complexes are unstable without gas impurities [26].

One cannot fail to note the numerical values of coefficients at concentrations of alloying elements and impurities in the parameter A (Eq. (1)) in Eqs. (2)–(4) to be the determining factor in the models suggested for explanation of the nature of RE in RPVS. Among the most often referenced works which address considerations of possible mechanisms of RE in RPVS are Refs. [3,6,27–31]. In Ref. [27], RE in American grade RPVS is explained by their radiation-induced hardening, mainly due to ultrafine dispersed segregation of Cu and also to other areas enriched with copper or copper-vacancy clusters. In Refs. [5,15,22,32] the mechanisms of RE in Russian RPVS were suggested. An important role in the processes of RE was attributed not only to hardening of steels under irradiation, but to grain boundary and intragranular segregation of impurities (mainly phosphorus) as well. In Ref. [32] two facts are pointed out: grain boundary phosphorus segregation is most valuable for RPVS 15Kh2NMFA, applied in the production of pressure vessels and its intragranular segregation, at irradiation temperatures < 100°C.

A common approach is to consider hardening resulting from irradiation as the determining mechanism of RE in actually applied RPVS both of American and Russian grades [3,22]. Forcible arguments exist supporting this conviction, in particular:

(i) All RPVS significantly harden under irradiation. As a rule, an increase in yield stress for RPVS after irradiation at ~ 240–290°C to neutron fluence $\leq 10^{24}$ n m^{-2} constitutes ~ 20–40% [5,22,33,34].

(ii) Density and sizes of radiation-induced precipitate populations and dislocation loops, which are usually considered to be related to hardening in RPVS under irradiation, grow with increase in neutron fluence [35,101].

(iii) After recovery annealing of irradiated RPVS, a decrease in $\sigma_{0.2}$ caused by irradiation occurs simultaneously with partial or complete recovery of ΔTT [5,36,37].

Several common features accompanying the phenomenon of RE in different RPVS imply a global explanation:

(i) The character of changes in transition curves caused by irradiation is the same for all RPVS. Practically in all cases, as shown in Fig. 1, they are shifted to higher

temperatures, changes in the slope within the region of DBTT and also a lowering of USE is observed [1,5].

(ii) The character of recovery of the shift in DBTT (ΔTT), the changes in yield stress and USE caused by irradiation and subsequent recovery during heat treatment at temperatures ≤ 500°C are rather similar for all RPVS [36–38].

(iii) The character of changes in transition curves caused by irradiation and subsequent recovery during heat treatment at temperatures ≤ 500°C is rather similar for all RPVS also. In all cases a downward shift of transition curves to lower temperatures, an increase in their slope in the region of DBTT and an increase in USE occur [36–38] (in some cases to higher than the initial values prior to irradiation).

However, the above similarities by themselves do not prove a dominant contribution of hardening to RE for RPVS. Some aspects of the experimental data obtained earlier and also of data obtained recently by other researchers indicate that hardening evidently is not the single cause and in some cases possibly is not the dominating mechanism of RE in RPVS.

In the present paper, experimental data are analyzed to assess the contribution to RE in RPVS from different mechanisms.

3. Experimental

The following American grade RPVS have been investigated under the auspices of the IAEA program on radiation embrittlement of reactor vessel steel:

- ASTM A533 type B class 1 steel plate, manufactured by Kawasaki Steel Corporation at Muzushima Works. After rolling, the plates were heat treated under the following conditions: normalizing: 900°C for 4.5 h, air cooling; quenching: 880°C for 3 h, water cooling; tempering: 665°C for 12 h, air cooling; simulated post weld heat treatment: 620°C for 40 h, furnace cooling. The designation of this steel is JRQ.
- ASTM A533 B class 1 steel welded joint. The designation is JWP.
- ASME A508 class 3 steel welded joint. The designation is JWQ.

The weld materials were manufactured by the Ibaraki Plant, Kobe Steel. Post weld heat treatment for the steels JWQ and JWP was: holding for 40 h at 620°C and furnace cooling.

Also the following Russian grade steels have been investigated:

- 15Kh2MFA base metal (WWER-440). After forging, the heat treatment was as follows: 1000°C/10 h, oil cooling; 700°C/16 h and air cooling.
- 15Kh2NMFA base metal (WWER-1000). Heat treatment: 920°C/1 h, water cooling, 650°C/20 h, air cooling, 620°C/25 h, 650°C/20 h and furnace cooling to room temperature.
- 25Kh3NM base metal (experimental PWR). Heat treatment: 870–890°C, air cooling to 700–800°C, oil quenching, tempering at 620–670°C and furnace cooling.
- SV-10KhMFT (WWER-440) weld metals. Post weld heat treatment: tempering for 15 h at 665°C and furnace cooling to 300°C.
- for the Russian weld metals: holding for 15 h at 665°C, furnace cooling to 300°C and then air cooling.

The chemical compositions of the above steels are presented in Table 1.

Embrittlement of the specimens after irradiation has been assessed from the DBTT shift and the decrease of upper shelf energy in impact tests of V-notch Charpy specimens. Fractographic examination has been carried out on broken halves of Charpy specimens, which were stored under vacuum after the tests, in order to preserve the fracture surfaces.

The fracture surfaces were examined using an X-ray microbeam analyzer type SXR-50, radioactive version (Cameca) that was installed in a protective chamber. The images of the fractures were obtained with secondary electrons at accelerating voltage 20 kV and probe current 0.8 nA with magnification in the range 50–3.500 $\times$. The fractions of different types of fracture (ductile, ductile intercrystalline, cleavage and quasicleavage) in the total fracture surface after the tests at different temperatures were evaluated using the Glagolev method [39]. The absolute error of measurements at 95% confidence level did not exceed 3%. Testing temperatures for each material corresponded to the upper shelf, DBTT and lower shelf in the temperature dependence of the absorbed energy.

An electron microscope type TEMSCAN-200CX was used for transmission electron-microscope (TEM) studies at an accelerating voltage of 200 kV. During determination of the densities of both radiation defects and precipitates, the specimen thickness in the electron transparent area was measured using the convergent beam electron diffraction method [98] with an accuracy exceeding 95%.

The specimens for TEM studies were cut from the halves of fractured Charpy specimens and prepared by electrolytic polishing using a Struers electropolisher with an electrolyte of 10% $HClO_4$ and 90% methanol at -60–-75°C.

The chemical composition of grain boundaries has been evaluated by secondary ion mass spectroscopy (SIMS) and Auger electron spectroscopy using a VG Escalab-5 instrument designed for combined analysis of the surface. Cylindrical specimens of 25 mm length and 4 mm in diameter with a ring notch 1 mm depth (notch radius 0.1 mm) have been tested. The specimens were brittle fractured using an impact bend at -170°C in a vacuum of 10^{-9} Torr inside the spectrometer chamber. The depth analyzed was 2.0–2.4 nm. Semiquantitative comparative analysis of the chemical composition has been carried out using Auger peak height

Table 1
Chemical composition of reactor pressure vessel materials investigated

Designation	ASTM code	Chemical composition (wt%)									
		Si	Mn	P	S	Cu	Ni	Cr	Mo	C	V
JRQ	A 533B class 1 Plate	0.24	1.42	0.017	0.004	0.14	0.84	0.12	0.51	0.19	0.003
JWP	A 533B class 1 Weld	0.33	1.18	0.009	0.004	0.03	0.9	0.06	0.03	0.09	0.002
JWQ	A 508 class 3 Weld	0.3	1.29	0.026	0.005	0.26	1.1	0.04	0.48	0.09	0.002
15Kh2MFA		0.27–0.37	0.39–0.48	0.011–0.016	0.012–0.018	0.12–0.14	0.19–0.27	2.52–3.00	0.64–0.71	0.13–0.18	0.25–0.31
SV-10KhMFT		0.15–0.35	0.97–1.03	0.029–0.036	0.012–0.013	0.15–0.21	0.09–0.21	1.37–1.58	0.43–0.50	0.05–0.07	0.19–0.23
15Kh2NMFA		0.23	0.42	0.009	0.008	0.09	1.25	2.14	0.59	0.16	0.10
25Kh3NM		0.44	0.49	0.024	0.018	0.10	1.02	3.03	0.40	0.23	–

ratio (phosphorus (120 eV) to iron peak (703 eV) [40]). Experimental data were averaged over 7–10 boundaries (facets) for grains of different orientations to diminish an influence of this factor on the data.

4. Results and discussion

The rationale adopted in the present paper is that in view of the complexity of the RE phenomenon in RPVS, an overview is required of existing published experimental data. Therefore, these data will first be presented along with the conventional interpretation. Then follow the new results together with interpretation based on existing and new philosophies.

Transition curves which are the same for all unirradiated RPVS and those transformed by irradiation are illustrated schematically in Fig. 1. The mechanism or mechanisms selected are required to explain all changes in the transition curve (impact strength) due to irradiation, if only qualitatively. These changes are as follows:

(i) the DBTT shift.

(ii) the decrease in slope in the ductile–brittle transition region.

(iii) the decrease in the USE.

Possible mechanisms that could lead to these three phenomena and which agree with available experimental data are now discussed.

4.1. The shift in ductile to brittle transition temperature

Three mechanisms are known that can, in principle, induce an upward shift of the transition temperature:

(i) hardening (increase in yield stress of steels).

(ii) grain boundary segregation (primarily from phosphorus).

(iii) impurity segregation (primarily from phosphorus) at precipitate/matrix interfaces, i.e., intragranular impurity segregation.

Griffith [102] was the first to explain the propensity of steels with a BCC-type crystal lattice to brittle fracture at lower temperatures. The explanation suggested essentially involved the temperature dependence of the yield stress (and ultimate stress) in these steels (Fig. 2).

Following the Griffith approach, brittle fracture in steel (at decreasing temperature and a simultaneous increase in yield stress) can occur when energy E_{def} accumulated from deformation becomes equal to (or exceeds) the energy necessary for formation of the free surface of a fracture (E_{srf}): $E_{def} \geq E_{srf}$, or

$$\sigma \varepsilon s l \geq \gamma s K, \tag{5}$$

where σ is the stress at the initial moment of cracking, s the area of the specimen section, l the length of its operating part, γ the surface energy of steel at testing temperatures and K the coefficient accounting for a relief of the fracture surface, $K > 1$.

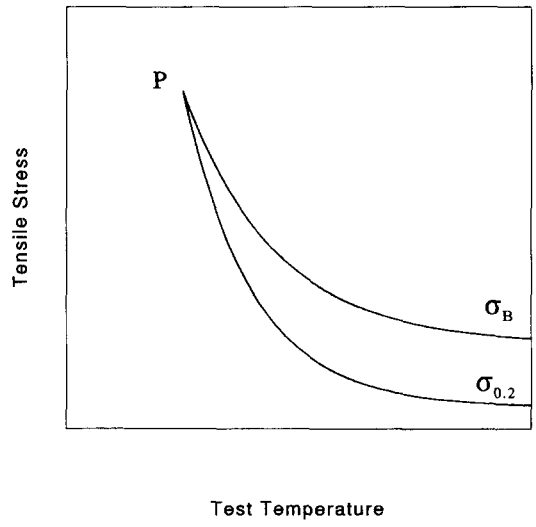

Fig. 2. Schematic showing temperature dependences of yield and ultimate tensile stress.

Actually an ideal brittle fracture cannot be realized even in the immediate vicinity of the point 'P', (Fig. 2), where the curves of temperature dependencies of ultimate and yield stresses intersect. At this point Eq. (5) has the form

$$\sigma_{0.2}\varepsilon_y sl \geq \gamma sK, \tag{6}$$

where $\sigma_{0.2}$ is the yield stress at the testing temperature corresponding to the point 'P' in Fig. 2, ε_y is the elastic deformation of the specimen and γ the surface energy at the testing temperature.

In all other cases the fracture is preceded by ductile deformation. So in the general case the absorbed energy (A) is

$$A = A_{\text{elst}} + A_{\text{dct}} + A_{\text{srf}}, \tag{7}$$

where A_{elst} is the contribution to A from elastic deformation:

$$A_{\text{elst}} = \sigma_{0.2}\varepsilon_y sl = \frac{\sigma_{0.2}^2}{E} sl. \tag{8}$$

Here E denotes the Young's modulus at the testing temperature and A_{srf} is the contribution to the absorbed energy, associated exclusively with formation of the free fracture surface:

$$A_{\text{srf}} = \gamma sK. \tag{9}$$

A_{dct} is the contribution concerning the ductile deformation preceding the specimen fracture that depends on the testing temperature, T:

$$A_{\text{dct}} = \int_{\varepsilon_\gamma}^{\varepsilon_0(T)} \sigma(\varepsilon, T)s(\varepsilon, T)l(\varepsilon, T)\varepsilon(T)\,\mathrm{d}\varepsilon, \tag{10}$$

where $\varepsilon_0(T)$ is the value of the material ductility at testing temperature and $\sigma(\varepsilon, T)$, $s(\varepsilon, T)$, $l(\varepsilon, T)$ and $\varepsilon(T)$ are the corresponding functions involving the dependence on testing temperature.

The Davidenkov diagram [103,104] is usually used to illustrate the phenomenon of the DBTT shift resulting from hardening (Fig. 3).

Based on this diagram, a vertical shift of temperature dependence of yield stress results, if an increase in the yield stress occurs for any reason. If the increase is caused by irradiation of RPVS, then the initial and final curves (1 and 2, respectively) are equidistant [24,25]. Thus, in the frame of the diagram, only an increase in DBTT may occur, that is its shift towards higher temperatures, due to an increase in the yield stress caused by any reason.

It is worth noting that in contradiction with Fig. 3, the stress of tearing, σ_{trn} (that is the true ultimate stress) depends on the temperature and decreases with increase in temperature [41,42]. The reason is that in steels with BCC lattice, the yield and ultimate stresses strongly depend on temperature. For example, in the base metal of a WWER-440 pressure vessel made from steel 15Kh2MFA, both in the initial state and after irradiation in conditions close to operating ones, the values of yield stress at -198 and 270°C differ by almost double. The difference between ultimate and yield stresses at 270°C constitutes ~ 25–30% (both before and after irradiation) and tends to zero at -198°C.

Analysis of representations inherent in the Davidenkov diagram and some additional considerations show that its principal corollary (that an increase in yield stress due to hardening and caused by any reason can induce only an increase in DBTT shift) is far from being indisputable. The diagram is based on the following principal proposition: absorbed energy in steel cannot be unchanged or increased (at a fixed testing temperature) by hardening.

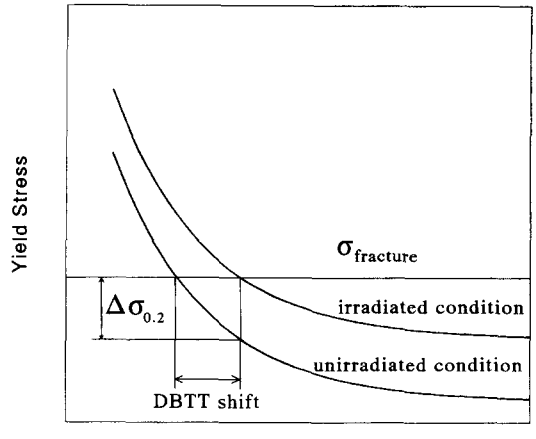

Fig. 3. Davidenkov's diagram.

If this proposition is not true (at a fixed testing temperature, for example, in the region of DBTT), then a shift will not be observed or temperature dependencies of both impact strength and ductile-to-brittle transition will be shifted downwards. The possibility of the absence of a shift or downward shift as a result of hardening is not possible in the frame of the Davidenkov diagram.

For this situation it would be interesting to consider the conditions when this situation might occur. From Eqs. (7), (8) and (10) one obtains the following formula for the absorbed energy at a fixed testing temperature (T):

$$A = \frac{\sigma_{0.2}^2(T)}{E(T)} sl + \int_{\varepsilon_\gamma(T)}^{\varepsilon_0(T)} \sigma(\varepsilon, T) s(\varepsilon, T) l(\varepsilon, T) \varepsilon(T) \times d\varepsilon + \gamma(T) s(T) K(T). \quad (11)$$

The dependence on T is emphasized in the expressions for $\sigma_{0.2}$, σ, E, s, l and K.

Let us see which terms in the right-hand side of Eq. (11) can yield the transition curve characteristic of steels with BCC lattice. The first term in this equation (A_{elst}) increases with a decrease in the temperature. The reason is that the yield stress increases almost double while the testing temperature changes from ~ 300 to 200°C. Young's modulus increases nearly 2–4% for every 100°C increase of the temperature [43]. Therefore, in this temperature range it increases by 20% at the most with a decrease in the temperature. It should be kept in mind that in accordance with Ref. [44] the value of Young's modulus within the limits of elastic deformation does not depend on the rate of the material deformation. Let us calculate the value of A_{elst} for Charpy specimens made from RPVS at −200°C that is deliberately within the lower shelf of the absorbed energy (but where A_{elst} has the maximum value within the range from −200 to +300°C). In these calculations the value of S has been assumed to be 8×10^{-3} m^2, $l \approx 2.5 \times 10^{-4}$ m (the curvature radius of the notches on Charpy specimens), $E = 212 \times 10^3$ MN/m^2 [45]. Numeric evaluation shows that in this case $A_{elst} \approx 0.5$ J, so it is one order of magnitude less than the typical value of absorbed energy on the lower shelf which is usually ~ 5 J.

The third term in Eq. (11), A_{srf}, may increase with a rise in test temperature due to the temperature dependence of γ (γ is independent on the deformation rate). However, the coefficient K, taking account of the degree of complexity of fracture surface, decreases with a decrease in testing temperature. Thus, the resulting change in A_{srf} occurring with a decrease in testing temperature is determined by the term γ. These considerations lead to the conclusion that the change in K due to the transition from a completely brittle fracture (on the lower shelf) to a completely ductile one (on the upper shelf) is insignificant. This evaluation can be simplified if one assumes that the specimen fracture (on the lower shelf) is a plane of area S coinciding with the specimen section and on the upper shelf this plane changes to a set of hemispherical dimples, which have the radius equal to the depth (100% ductile fracture). This assumption is realistic, as the direct observations of dimples on ductile fractures and also the values of the sharpness characteristic of raster electron microscopy show. If one also assumes that these dimples have the same radius r, then the ratio of the fracture area on the upper shelf to the area on the lower shelf can be approximately represented as

$$S_{US}/S_{LS} = S2\pi r^2/\pi r^2 S = 2. \quad (12)$$

It can be seen from Eq. (12) that the ratio does not depend on r (dimple radius). Also, it follows that the values of K and A_{srf} rise approximately by double while the testing temperature changes from the lower to upper shelf (for instance from −200 to +300°C). If one assumes the second term in Eq. (11) $A_{dct} \approx 0$ (for instance at such temperatures that $\sigma_{0.2} = \sigma_b$) in the region of the lower shelf, then clearly the value of A_{srf} is either less than the absorbed energy at the lower shelf or commensurable (in the region of the lower shelf). Direct evaluation of A_{srf} may be produced from the data in Refs. [41,42]. In these studies the value of the surface energy for α-Fe at 20°C is given. Moreover, $\gamma = 2.09$ J/m^2. For each 100°C of temperature increase, γ decreases by nearly 10% [41,42]. $S = 0.8 \times 10^{-4}$ m^2 for a standard Charpy specimen. Respectively, $A_{srf} = 1.67 \times 10^{-4}$ J for the Charpy specimen and thus, throughout the entire range of testing temperatures, A_{srf} is well below the absorbed energy at the lower shelf, which is usually ~ 5 J. Moreover, if one takes into account that the typical ratio of the values of the absorbed energy at the upper and lower shelves is of ~ 20 J or more, then the following conclusion can be drawn: the temperature dependence of the absorbed energy for steels is determined practically exclusively by the value of A_{dct} in Eq. (11).

So, the analysis of the second term in Eq. (11) or Eq. (10) gives the conditions providing the increase in the absorbed energy induced by hardening. The term under the integral sign in Eq. (10) looks rather complicated, but as seen from Ref. [46], the functions S and l can be assumed constant at the ductility level < 10% (that nearly corresponds to ductility levels characteristic of RPVS). Assuming this is true, one obtains the following condition for the values of the absorbed energy to be conserved or increased when hardening is observed:

$$\sigma_1^* \varepsilon_1 \le \sigma_2^* \varepsilon_2, \quad (13)$$

where σ^* is the strength of ductile deformation, $\sigma_{0.2} < \sigma^* < \sigma_b$, σ_1^* is prior to hardening and σ_2^* after hardening ($\sigma_1^*/\sigma_2^* < 1$). ε_1 and ε_2 are the material ductility prior to and after hardening, respectively. Eq. (13) can be rewritten as

$$\Delta\sigma/\sigma \ge \Delta\varepsilon/\varepsilon, \quad (14)$$

where $\Delta\sigma/\sigma$ is the relative radiation induced increase of

yield stress and $\Delta\epsilon/\epsilon$ is the relative radiation induced decrease of ductility.

Moreover, it should be kept in mind that hardening in steels and alloys caused, for example, by heat treatment may induce a rise in ductility [47]. So, in a general case, the Davidenkov diagram is improper for interpretation of the hardening influence on metals (steels) with a BCC lattice.

Therefore, the analysis of specific changes in yield (ultimate) stress for different RPVS irradiated in conditions typical of WWER and PWR is of prime interest.

The major part of experimental data on the influence of irradiation on strength and ductility properties of RPVS was obtained from tensile testing of specimens. It was shown in Ref. [48] that irradiation of American and Russian RPVS to neutron fluences $\leq 10^{24}$ n m^{-2} induces, as a rule, the hardening phenomena and a simultaneous decrease in ductility. Moreover, as a rule, Eq. (13) is satisfied. If it was possible to transfer the properties of RPVS obtained in tensile testing to impact, then one could obtain an increase in the absorbed energy as a result of hardening over all testing temperatures from ~ -100 to $+270$°C. But it is well known that this is not observed in practice. Fig. 4 shows the typical temperature dependencies of yield and ultimate stresses, uniform and total elongation of specimens made from steel 15Kh2MFA (after tensile testing) before and after irradiation.

Fig. 4 shows that in the range -198 to $+270$°C, both the uniform and total elongation in steel are practically unchanged. In comparison, in the same range, the significant rise in yield and ultimate stresses with decreasing temperature occurs. This behaviour of the strength and ductile properties of RPVS in tensile testing does not explain and even contradicts the character of temperature dependencies of impact strength in the same temperature range and in the same materials, where the absorbed energy decreases from the upper to the lower shelf. Obviously, the ductile and strength properties of RPVS measured in tensile testing are essentially different from the corresponding values measured in impact testing. First of all, this is due to the large difference in the rates of deformation in these two types of testing. In impact testing, the rates of deformation are approximately 10^5–10^6 times greater. Likewise, it is evident that at high rates of deformation (at decreasing testing temperature) ductility ought to decrease, beginning from significantly higher temperatures, than in tensile testing. Apparently, the rise in deformation rate changes the character of influence of some processes on ductility. For instance, in tensile testing, the presence of grain boundary phosphorus segregation does not influence on elongation [49,50], but at high deformation rates (characteristic of impact testing) undoubtedly does. Otherwise, impact testing would not demonstrate the shifts of transition curves due to temper brittleness. As follows from Eq. (11), it is impossible to get a high decrease in the absorbed energy without a

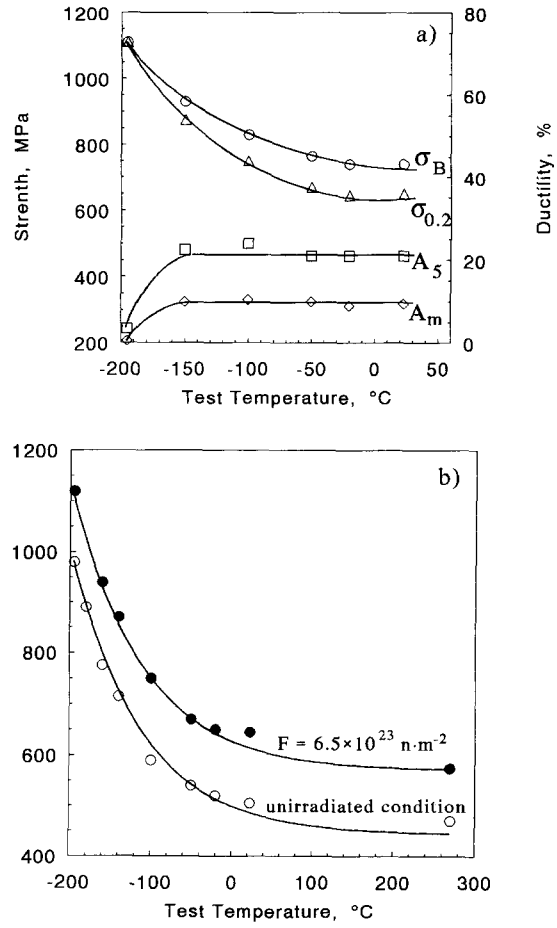

Fig. 4. Temperature dependence of the tensile properties of 15Kh2MFA steel. Private data of V.A. Nikolaev [48]. (a) Irradiated material; (b) comparison of unirradiated and irradiated conditions of the steel.

catastrophic decrease in ductility. Analysis of the data obtained in instrumented impact testing demonstrates that the rate of loading strongly (as compared to tensile testing) influences the measured values of ultimate and yield stresses. It should be taken into account when analyzing experimental data. By now, a great deal of publications are available where the results obtained in tensile testing (or some other 'slow' types of loading, e.g., measurements of hardness) are applied to analysis, interpretation or development of RE models basing on impact testing [3,28,51]. In these works, similar to the Davidenkov diagram, it is assumed that the processes leading to a rise in $\sigma_{0.2}$ inevitably induce an upward shift in DBTT. For this reason, this model as well as ones mentioned above involve the value of $\Delta\sigma_{0.2}$ instead of ΔTT. As shown above, the application of $\Delta\sigma_{0.2}$ instead of ΔTT cannot be validated. In addition, the second term in Eq. (11) provides only an

increase in the value of A_{dct} with an increase in $\sigma_{0.2}$ due to hardening. A decrease in the second term may be caused only a by decrease in ductility, which is proportional to $(\sigma_b - \sigma_{0.2})$. These facts indicate that the experimental correlation observed between the values of $\Delta\sigma_{0.2}$ and ΔTT is not universal and the conditions under which they can be applied are not determined even for the studied materials. Some examples will be given below.

Therefore, an extraction of contributions to RE of RPVS from different mechanisms (e.g., hardening) is an extremely complicated problem. Different mechanisms of RE can behave differently in different regions of the transition curve (e.g., within the upper shelf or DBTT). It has been pointed out earlier that irradiation of RPVS results in a number of microstructural phenomena and each of them can induce RE. Therefore, to evaluate the possible influences of different mechanisms on variations in the transition curve it would be reasonable to examine the separate contributions from each one.

It is convenient to consider the hardening effect on RE by taking experimental studies devoted to cold deformation of steels as an example. The influence of cold deformation on strength and ductility of steels is studied well enough, e.g., Refs. [52,53]. However, the number of studies involving its influence on impact strength in steels is rather low [54–64]. As a rule, the authors of such publications only confirm that cold work decreases the absorbed energy in impact testing [54]. But detailed analysis of the experimental data from the publications leads to the conclusion that actually the influence of cold deformation on the impact strength in steels is rather complicated.

For instance, in Ref. [58] it is demonstrated that cold deformation may induce the rise in absorbed energy in some steels. In steel S55C the absorbed energy increases slightly with an increase in cold deformation to 20% and after that it drops sharply with the increase in deformation to 30%.

In Refs. [60,61,99], very interesting data were obtained on the studies of the influence of cold deformation in steel St.3 (0.15% of carbon) and α-Fe (0.027% C, 0.18% Mn, 0.2% Si, 0.025% S, 0.006% P) on DBTT, yield stress and other parameters. In Fig. 5 the data from Refs. [60,61] are plotted. From these data it is seen that cold deformation is accompanied by the rise in yield stress, so at first material hardening induces the rise in DBTT, then it does not influence the level of DBTT and, lastly, it even leads to reduction of DBTT at high degrees of cold deformation.

Similar results were obtained in studies on the influ-

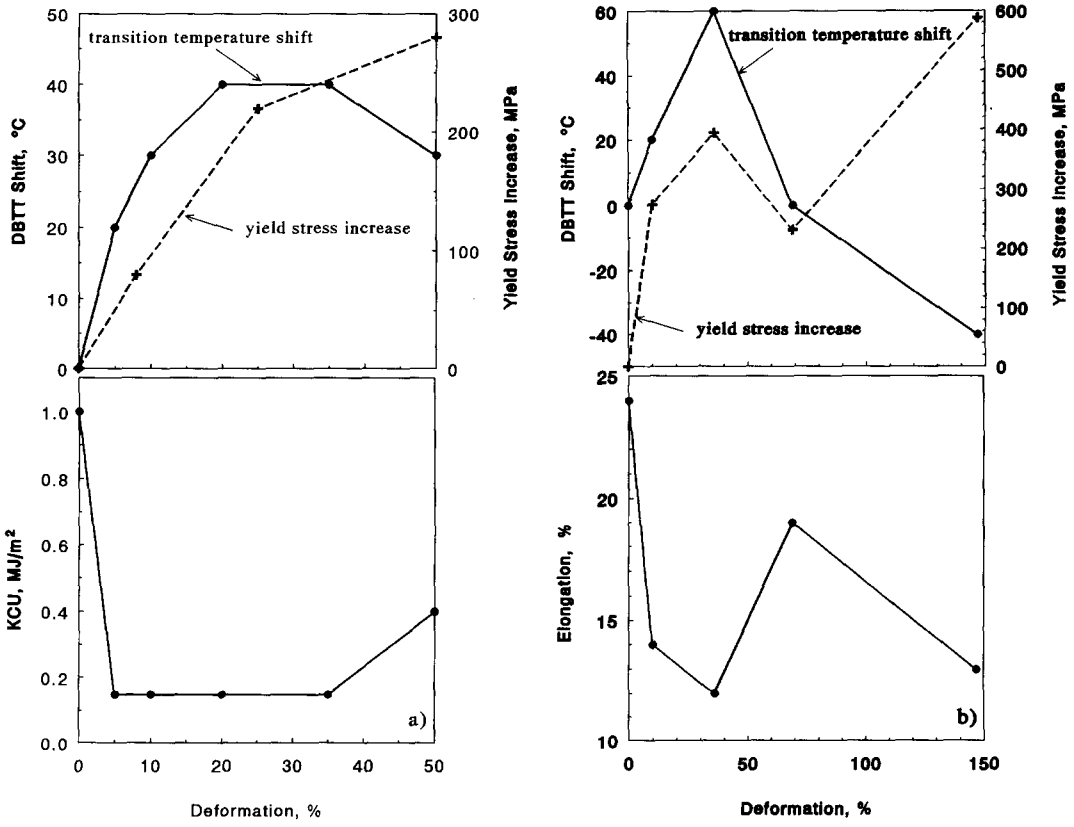

Fig. 5. Dependence of the mechanical properties of St.3 steel (a) and α-Fe (b) on degree of cold deformation [60,61,99].

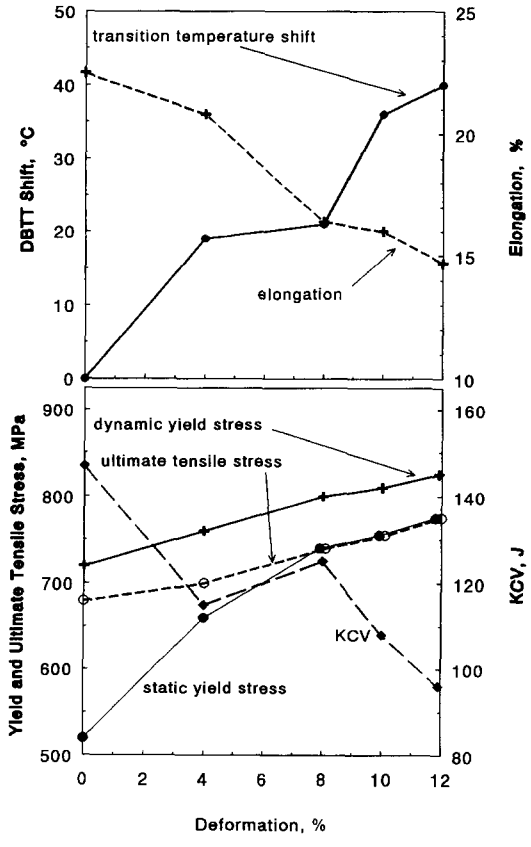

Fig. 6. Dependence of the mechanical properties of A533B steel on degree of cold deformation [63].

ence of cold deformation on the properties of RPVS A533B [63]. Many parameters were measured there including DBTT, yield stress, ductility and some others. In Fig. 6 some of the obtained dependencies are plotted. In particular, it can be seen from these dependencies that a monotone increase in the yield stress of steel A533B with an increase in the degree of cold deformation is not always accompanied by a proportional rise in DBTT.

The following fact attracts considerable attention: in Refs. [60,61,63] the values of relative hardening resulting from cold deformation in steels significantly exceed the typical ones of WWER and PWR. For instance, the maximum value of relative rise in the yield stress is ~ 100% for steel St.3 and ~ 55% for steel A533B. The DBTT shift is, respectively, ~ 40 and ~ 50°C. Usually the values of relative change in the yield stress do not exceed ~ 40%. Moreover, radiation-induced DBTT shifts can reach ~ 150–200°C and even greater values [5]. So, when hardening is caused by cold deformation in steels, the resultant DBTT shifts are a few times less than the shifts induced by irradiation of RPVS.

Summarizing the data published on the influence of cold deformation on impact strength in steels, the following can be noted:

(i) hardening in steels due to cold deformation can induce an upward shift in DBTT.

(ii) the rise in the yield stress due to cold deformation is not always accompanied by the rise in both absorbed energy and DBTT. Therefore, the considerations forming the basis of the Davidenkov diagram as well as the diagram itself are not universal.

(iii) the data show that the changes in DBTT for steels cannot be predicted even qualitatively based only on hardening.

The studies discussed do not include data on ductility in steels observed before and after cold deformation at the deformation rates typical of impact testing. But from Eqs. (10) and (11) and also previous discussions one can see that the deformation has to induce a shift in temperature dependencies of ductility at these rates. The temperature dependencies (in contrast with obtained in tensile testing) have to be similar to the corresponding transition curves in the range of temperatures specific for impact testing (Fig. 7).

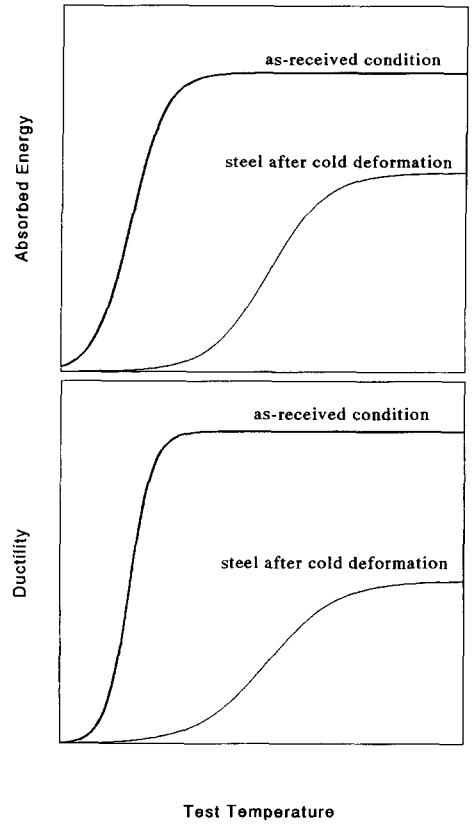

Fig. 7. Influence of cold deformation on impact energy and material ductility at deformation rates typical of impact Charpy testing.

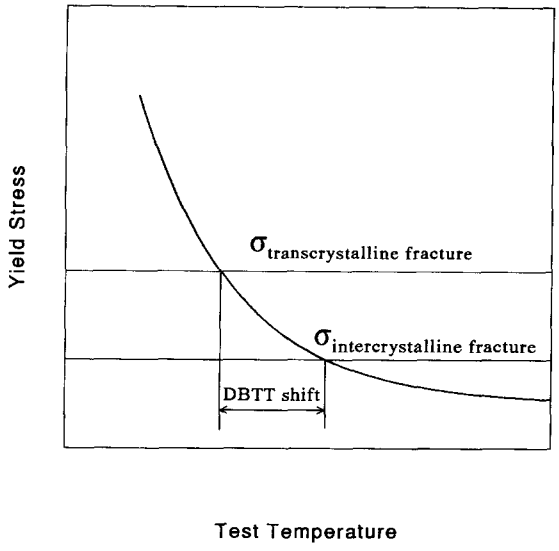

Fig. 8. Schematic mechanisms of DBTT shift in steel with BCC lattice due to grain boundary segregation of impurities.

Qualitatively this consideration can be confirmed using the data on lateral expansion of Charpy specimens due to impact testing.

The mechanism of the DBTT shift due to grain boundary segregation of impurities is usually illustrated with the use of the diagram in Fig. 8.

In compliance with this diagram, the shift appears when the stress of tearing of the crystalline boundary ($\sigma_{\text{inter.trn.}}$, intercrystalline tearing) becomes equal or less than the stress of tearing inside crystallites ($\sigma_{\text{trans.trn.}}$, transcrystalline tearing):

$$\sigma_{\text{inter.trn.}} \leq \sigma_{\text{trans.trn.}}; \tag{15}$$

Moreover, the greater the difference between $\sigma_{\text{trans.trn.}}$ and $\sigma_{\text{inter.trn.}}$, the greater the value of the temperature shift (Fig. 8).

This scheme involves the assumption that grain boundary segregation of impurities cannot facilitate an increase in ductility of steels, i.e., finally, an increase in the absorbed energy. The published data on the influence of this kind of segregation on mechanical properties ($\sigma_{0.2}$, σ_b and δ) of steels were obtained mainly in tensile testing. As pointed out above, tensile testing has not revealed an influence of grain boundary phosphorus segregation on yield stress, ductility and other properties, except the relative reduction of the area [50]. They do not deliver adequate representation of changes of properties occurring at deformation rates typical of impact testing. But in distinction from hardening, there are no data supporting the assumption that grain boundary segregation could induce a rise in ductility. As well, there are no examples where grain boundary segregation of impurities (e.g., phosphorus) induced downward shift in the transition curves. These facts do not permit to prove the character of the scheme considered is universal in all cases involving grain boundary segregation of impurities, but they also do not permit to cast some doubt on it.

It was demonstrated in a few studies that reduction of cohesion at grain boundaries (i.e., reduction of $\sigma_{\text{inter.trn.}}$) is closely connected with the level of impurity concentration in grain boundary segregation [65,66]. The condition $\sigma_{\text{inter.trn.}} \leq \sigma_{\text{trans.trn.}}$ is realized if the definite level of impurity concentrations is reached in the grain boundary segregation. In this case, in fractures of steel specimens, the areas appear with specific intercrystalline fractures [11,66–68]. At lower concentrations of impurities at grain boundaries, the intercrystalline component of the surface fracture and ΔTT associated with it are not observed. The considerations above allow the assumption that at least ductility in high-rate testing in the region of DBTT and lower shelf temperatures is sensible to the presence of grain boundary segregation. It seems likely that similar to cold deformation, grain boundary phosphorus segregation has to induce a shift of temperature dependencies of ductility for deformation rates characteristic of impact testing. These dependencies have to reproduce qualitatively the corresponding transition curves in the range of impact testing temperatures (Fig. 9).

It is pertinent to note that in distinction to Fig. 9, $\sigma_{\text{trans.trn.}}$ (as well as $\sigma_{\text{inter.trn.}}$) depends on the temperature. This is evident from the fact that as a rule in materials with grain boundary phosphorus segregation the fraction of the regions with intercrystalline fracture in specimen fracture surfaces is zero at the upper shelf, maximum at testing temperatures slightly lower than DBTT and diminishes with the further decrease in temperature (Table 2 and Ref. [69]).

The temperature range of the most intensive formation of temper embrittlement (formation of grain boundary

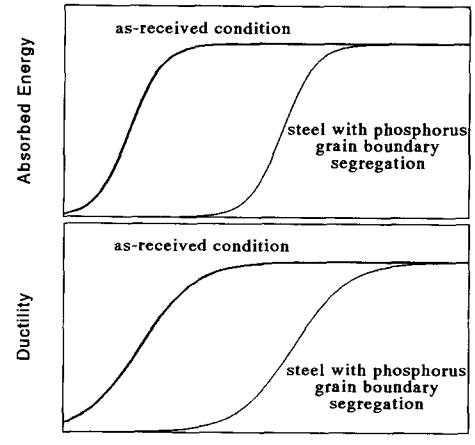

Fig. 9. Schematic influence of grain boundary segregation on temperature dependences of absorbed energy and steel ductility under deformation rates characteristic for impact testing.

Table 2
Summary data of fractographic analysis results for investigated Charpy specimens

N	Material	Material and specimen types	NPP unit	Fluence (10^{23} n m^{-2})	Condition	Test temperature (°C)	DBTT (°C)	Absorbed energy (J)	USE (J) curve	Position on the KVC–*T*	Fraction of different fracture modes (%)				
											ductile	quasi-cleavage	cleavage	intergranular	ductile intergranular
1	2	3	4	5	6	7	8	9	10	11	12	13	14	15	16
1	A533B 0.017% P 0.14% Cu	BM mini Charpy	research spec., irr. in WWER-440	–	unirrad.	−100	−25	1	22	LS	0	–	100	–	–
2				–		−25		3		DBT	15	–	85	–	–
3				–		100		22		US	100	–	–	–	–
4	A533B 0.017% P 0.14% Cu	BM Charpy	research spec., irr. in WWER-440	2.6	irrad.	100	70	83.1	128	DBT	40	–	40	10	10
5	A533B 0.017% P 0.14% Cu	BM Charpy	research spec., irr. in WWER-440	2.6	irrad. + anneal.	40	25	93.3	186	DBT	55	–	35	10	–
6	A533B 0.017% P 0.14% Cu	BM Charpy	research spec., irr. in WWER-440	10	reirrad.	100	130	19.6	108.2	LS	30	–	60	10	–
7						140		55.7		DBT	35	–	50	10	5
8						220		108.2		US	90	–	–	–	10
9	A533B 0.009% P 0.03% Cu	WM Charpy	research spec., irr. in WWER-440	10	reirrad.	−40	−15	16.5	150	LS	5	30	65	–	–
10						−20		26.7		DBT	15	35	50	–	–
11						20		152.9		US	80	15	–	–	5
12	A508 0.026% P 0.26% Cu	WM Charpy	research spec., irr. in WWER-440	10	reirrad.	40	110	4.7	128	LS	5	75	–	20	5
13						120		55.7		DBT	45	25	–	20	10
14						200		127		US	135	–	–	–	15
15	25Kh3NM 0.024% P 0.10% Cu	BM Charpy	cover from experiment, PWR	–	60 000 h thermal aging	−150	−22	5.4	191	LS	–	35	–	65	–
16						−35		46		DBT	10	5	5	65	15
17						100		191		US	85	–	–	–	15
18	25Kh3NM 0.024%Cu P 0.10% Cu	BM Charpy	cover from experiment, PWR	–	60 000 h thermal aging + anneal. 650°C/2 h	−175	−50	4.4	174	LS	–	50	5	45	–
19						−25		53		DBT	25	25	5	40	5
20						200		158		US	95	–	–	–	5
21	25Kh3NM 0.024% P 0.10% Cu	BM Charpy	Trepan from experiment, PWR	1.75	irrad.	−50	80	7.3	116	LS	5	15	5	70	5
22						88		45		DBT	30	5	5	50	10
23						250		116		US	90	–	–	–	10
24	25Kh3NM 0.024% P 0.10% Cu	BM Charpy	Trepan from experiment, PWR	5.05	irrad.	23	107	5	113	LS	5	20	–	70	5
25				3.7		175		40		DBT	40	5	5	40	10
26				3.7		225		90		US	90	–	–	–	10

27	Sv-10KhMFT 0.034% P 0.155% Cu	WM Charpy	Trepan from WWER-440	6.5	irrad.	−50	145	4.2	81.3	LS	5	95	–	–	n/d
28						125		43		DBT	60	40	–	–	n/d
29						213		72		US	90	10	–	–	n/d
30	Sv-10KhMFT 0.034% P 0.155% Cu	WM mini Charpy	Trepan from WWER-440	6.5	irrad.	−50	71	1.4	11.5	LS	10	70	15	5	n/d
31						50		4.2		DBT	40	40	10	10	n/d
32						250		11.5		US	100	–	–	–	n/d
33	Sv-10KhMFT 0.034% P 0.155% Cu	WM Charpy	Trepan from WWER-440	6.5	irrad. + anneal. 475°C/150h	−25	48	10	103	LS	15	65	20	–	n/d
34						50		65		DBT	75	15	10	–	n/d
35						150		90		US	100	–	–	–	n/d
36	15Kh2MFA 0.017% P 0.17% Cu	BM mini Charpy	Templ. from WWER-440	9.2	irrad.	−100	−25	0.4	6.6	LS	5	30	50	15	n/d
37						−25		2.6		DBT	20	20	45	15	n/d
38						200		6.6		US	100	–	–	–	n/d
39	15Kh2MFA 0.017% P 0.17% Cu	BM mini Charpy	Templ. from WWER-440	9.2	irrad. + anneal. 475°C/150 h	−100	−49	0.8	6.0	LS	5	80	–	15	n/d
40						−60		1.1		DBT	5	50	20	25	n/d
41						200		6.0		US	100	–	–	–	n/d
42	Sv10KhMFT 0.0375 0.18% Cu	WM mini Charpy	Templ. from WWER-440	6.7	irrad.	−50	91	0.4	9.6	LS	10	75	10	5	n/d
43						150		8.2		DBT	80	10	5	5	n/d
44						250		9.6		US	100	–	–	–	n/d
45	Sv10KhMFT 0.0375% P 0.18% Cu	WM mini Charpy	Templ. from WWER-440	6.7	irrad. + anneal. 475°C/150 h	−50	11	1.5	14.4	LS	15	75	5	5	n/d
46						25		7.7		DBT	30	50	15	5	n/d
47						250		14.4		US	100	–	–	–	n/d
48	Sv10KhMFT 0.0375% P 0.18% Cu	WM mini Charpy	Templ. from WWER-440	6.7	irrad. + anneal. 560°C/150 h	−50	−24	2.9	15.2	LS	20	65	10	5	n/d
49						−37		6.7		DBT	30	40	25	5	n/d
50						150		15.2		US	90	5	–	5	n/d
51	15Kh2NMFa 0.009% P 0.09% Cu	BM Charpy	res. spec. WWER-1000	...	unirrad.	−100	−20	3	130	LS	–	70	30	–	n/d
52						−25		45		DBT	50	50	–	–	n/d
53						100		120		US	100	–	–	–	n/d
54	15Kh2NMFA 0.009% P 0.09% Cu	BM Charpy	res. spec. WWER-1000	5	irrad.	−100	60	2.5	90	LS	–	65	20	15	n/d
55						55		40		DBT	55	35	–	10	n/d
56						100		87		US	100	–	–	–	n/d
57	15Kh2NMFA 0.009% P 0.09% Cu	BM Charpy	res. spec. WWER-1000	5	irrad. + anneal. 480°C/50 h	−20	0	8.5	147	LS	–	70	–	30	n/d
58						10		55		DBT	50	35	–	15	n/d
59						80		100		US	80	20	–	–	n/d

BM: base metal; WM: weld metal; LS: lower shelf; DBT: ductile to brittle transition region; US: upper shelf; n/d: not determined.

phosphorus segregation) is ~ 450–550°C [70–72]. These temperatures are ~ 200°C higher than the operating ones in WWER and PWR. As a consequence of this, for a long time, the grain boundary phosphorus segregation in RPVS during operation was believed to be unlikely. But the evaluations in some papers [11,15] demonstrated that in irradiation conditions typical of WWER or PWR the radiation-induced diffusion of phosphorus can lead to such phenomena in RPVS. Later on, it was revealed in investigations of irradiated American and Russian RPVS that grain boundary phosphorus segregation may occur (Fig. 10). In fracture surfaces of such Charpy specimens, the regions with an intercrystalline type of fracture may appear (Fig. 11). Table 2 shows the data of fractographic examination of some RPVS of American and Russian grades. It should be emphasized that in Russian RPVS, irradiation

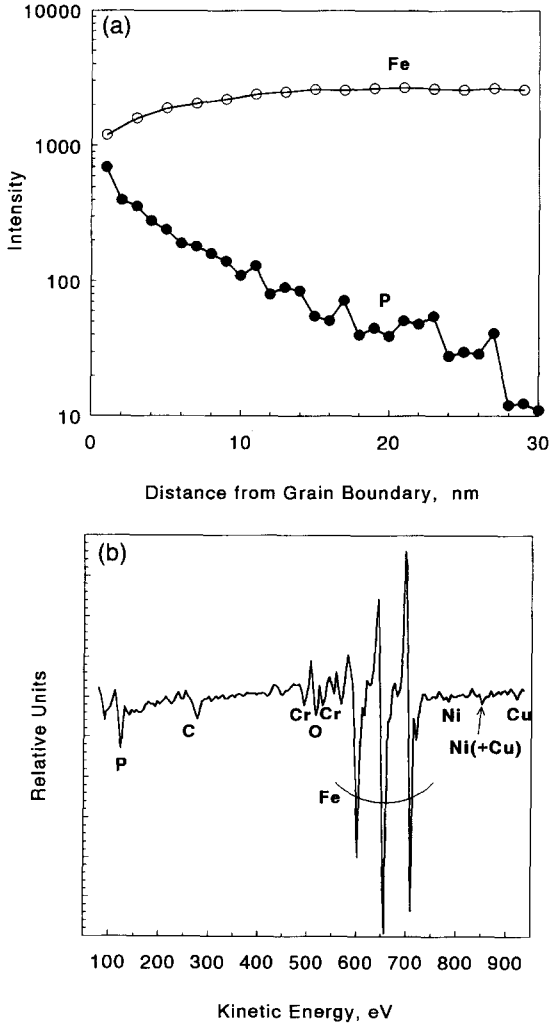

Fig. 10. Grain boundary phosphorus segregation observations. (a) Elements distribution in the vicinity of grain boundaries of irradiated WWER-440 base metal (SIMS results) and (b) typical Auger spectrum of irradiated nickel-alloyed RPVS.

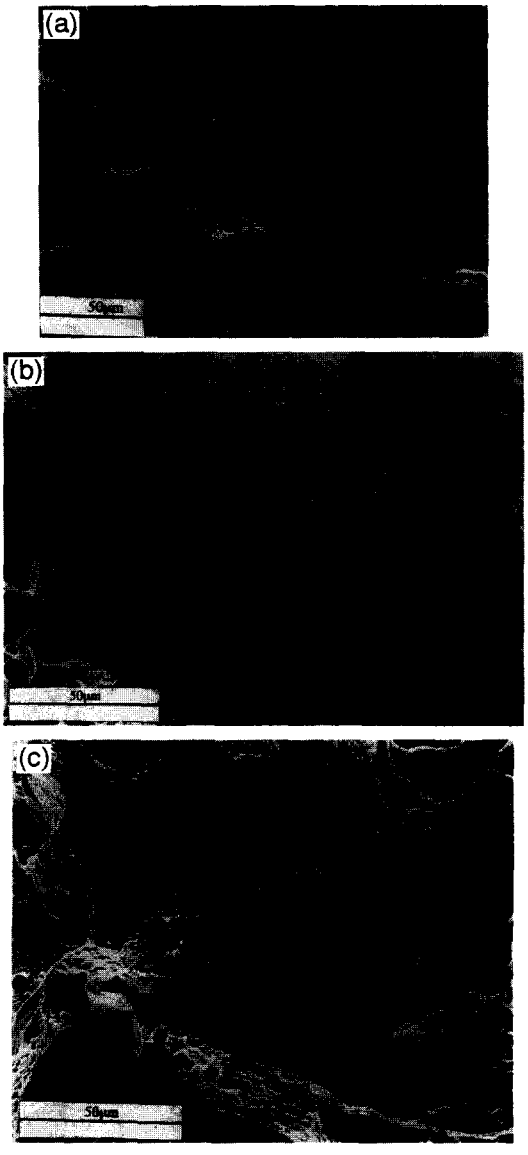

Fig. 11. Intergranular fracture in irradiated materials (fracture surfaces of Charpy specimens). (a) JRQ steel (T_{test} = 100°C); (b) trepan from weld of Russian experimental PWR (T_{test} = 50°C); (c) trepan from WWER-1000 base metal (T_{test} = − 100°C).

induces intercrystalline fracture only in base metal specimens. In irradiated weld metal this type of fracture was obtained only in sub-size Charpy, although in that metal the phosphorus content is greater (in standard Charpy an intercrystalline fracture was actually absent) [1].

[1] These distinctions in properties of irradiated standard and subsize Charpy specimens are evidently determined both by distinctions in characteristics of stress deformation state and deformation rates typical of impact testing of these two types of specimens.

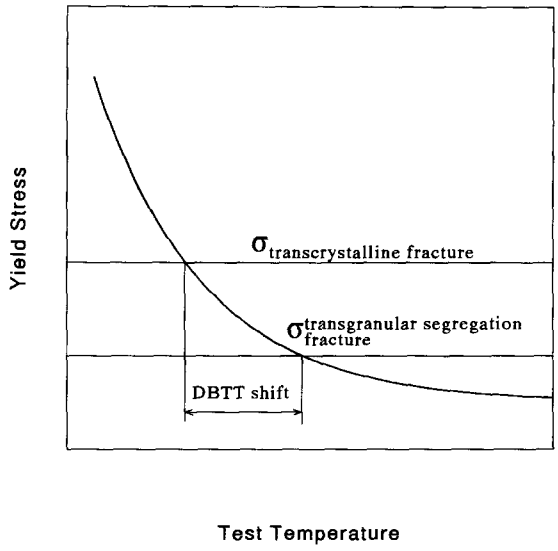

Fig. 12. Schematic mechanisms of DBTT shift in steel with BCC lattice due to intragranular segregation of impurities.

Apparently the distinction in the behaviour of base and weld metals of Russian RPVS can be explained by distinctions in the structure and properties of the grain boundaries.

Fractographic investigations (Table 2) indicate that irradiation can induce intercrystalline fracture in American RPVS as well (both in base and weld metals).

Available data provide support for the assumption that irradiation of RPVS of both grades in conditions specific of PWR is attended primarily with grain-boundary phosphorus segregation. This assumption is supported by direct observations carried out with the use of Auger spectroscopy, FEGSTEM and APFIM [10,11,73].

Fig. 12 illustrates the qualitative mechanism of DBTT shift (ΔTT) induced by intragranular segregation. This shift appears, if the effective stress of tearing due to intragranular segregation ($\sigma_{\text{eff.intra.}}$) diminishes below the true ultimate stress of transcrystalline fracture ($\sigma_{\text{trans.trn.}}$). Evidently, intragranular segregation is most probable at precipitate/matrix interfaces. But such segregation is probable also on various types of clusters, for instance, copper-vacancy clusters, radiation defects etc. This means that intragranular segregation, in contrast with that at grain boundaries, does not form continuous segregation surfaces where a crack can propagate. Therefore, to satisfy the relationship $\sigma_{\text{eff.intra.}} < \sigma_{\text{trans.trn.}}$ in the case of intragranular segregation, it is necessary to fulfil the following two conditions:

(i) the concentration of phosphorus in intragranular segregation (e.g., at precipitate/matrix interfaces) has to reach some specific value. After that, tearing along such an interface becomes preferential compared to transcrystalline fracture.

(ii) the ratio of medium diameter of precipitate (on which interface the phosphorus segregation emerges) to medium distance between them has to exceed a definite value, then their presence will induce the valuable reduction of true ultimate stress in steel (or $\sigma_{\text{eff.intra.}}$). It seems likely that $\sigma_{\text{eff.intra.}}$ is a temperature dependent value, as are $\sigma_{\text{trans.trn.}}$ and $\sigma_{\text{inter.trn.}}$. But the character of this dependence is yet to be explored, for the shortage of experimental data.

At the present time, papers are being published where direct experimental demonstrations of phosphorus segregation on interfaces of precipitate/matrix type and rise in DBTT due to intragranular phosphorus segregation inside steel are performed. For example, in Ref. [74] the segregation of this type was observed in RPVS A533, A508 and some model steels. Noteworthy is that intragranular segregation occurred there as a consequence of thermal aging at different temperatures. In Ref. [75] the experimental distinction of the phenomena such as hardening, grain boundary and intragranular phosphorus segregation that are observed during thermal aging and determine different contributions to the DBTT shift was gained. In Refs. [74,75], it was demonstrated that in RPVS and model steels the intragranular phosphorus segregation occurs mainly to precipitates of carbides of M_6C type, Laves phases and non-metallic inclusions. Furthermore, it was shown there that if any type of the above precipitates is located along the grain boundaries, then phosphorus segregation to their interfaces can lead to emergence of regions with ductile intercrystalline fracture in the fracture surfaces of Charpy specimens tested at temperatures of the upper shelf and DBTT. The ductile intercrystalline character of fracture has been observed by the current authors also in studies of fractures in Charpy specimens made from steel 25KhNM irradiated with a neutron fluence of $\sim(2\text{–}7)\times10^{23}$ n m^{-2} ($E > 0.5$ MeV) at 270°C after thermal aging at the same temperature during 60,000 h (Fig. 12 and Table 2) and also American grade steels A533B and A508 irradiated to neutron fluence 5×10^{23} n m^{-2} ($E > 0.5$ MeV) at 270°C (Fig. 13a, Table 2).

The phenomena related to intragranular segregation were found out when the studies of RE in some model binary alloys, Fe–P and Fe–Sn, were performed [76]. The influence of concentration of the second element on RE resulting from neutron irradiation to fluence $(3\text{–}5)\times10^{23}$ n m^{-2} ($E > 0.5$ MeV) at 50°C was studied in a series of binary alloys, Fe–Ta, Fe–W, Fe–Nb, Fe–Ti, Fe–Cu, Fe–P and Fe–Sn, in Ref. [76]. It was shown therein that in all the irradiated alloys, including the alloys Fe–Cu, but excluding Fe–P and Fe–Sn, the yield stress and DBTT as functions of concentration have the same shape. Fig. 14 presents the experimental dependencies from Ref. [76].

The important feature of these experiments is an absence of regions with intercrystalline fracture in the fracture surfaces of the specimens which have undergone impact testing. The opinion of the authors of Ref. [76] is

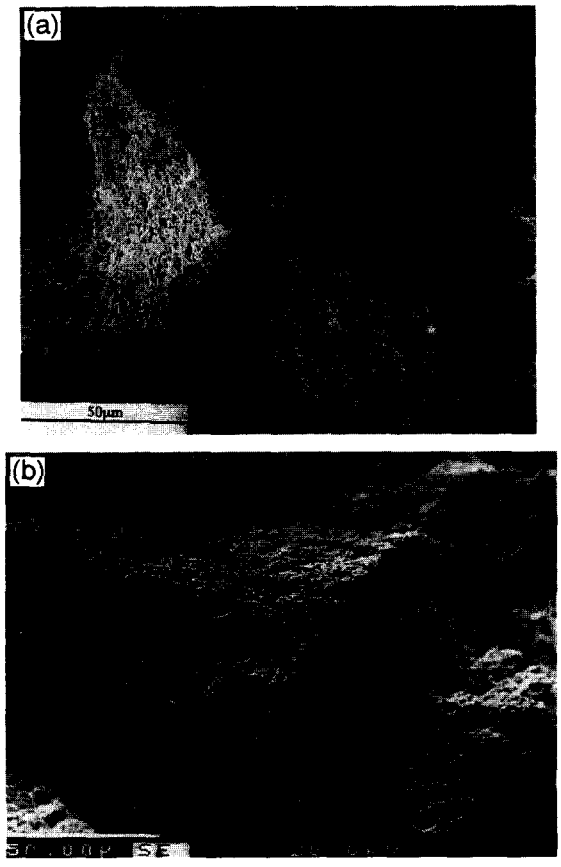

Fig. 13. Ductile intergranular areas on the fracture surfaces of irradiated Charpy specimens. (a) JRQ steel, test temperature corresponding to DBTT (100°C); (b) templet from Russian PWR, test temperature corresponding to upper shelf (225°C).

that this fact clearly indicates the dominating role of intragranular segregation in RE occurring in binary alloys Fe–P and Fe–Sn.

In Refs. [11–13,77] the intragranular phosphorus segregation was observed in steels of Russian and American grades irradiated in conditions characteristic of operating PWR with the use of direct experimental methods.

To summarize, the following conclusions may be drawn: the experimental data accumulated in studies of RPVS show that irradiation can induce grain boundary and intragranular segregation of impurities (primarily, phosphorus) as well as hardening. Moreover, each of these phenomena can induce an upward shift in the transition curve.

4.2. Reduction of the slope of the transition curve in the region of DBTT

Geometrical considerations permit us to deduce the following reasons for reduction of the slope:

(i) the change of the temperature interval between the right end of the lower shelf and the left end of the upper shelf in the transition curves.

(ii) the change of the upper shelf level in the curves.

(iii) simultaneous change of the parameters from items (i) and (ii).

As in Section 4.1, we consider the possible influence of hardening caused by grain boundary or intragranular segregation of impurities (chiefly phosphorus) on the slope.

From the data given in Section 4.1, one can see that irradiation of RPVS can produce complicated phenomena concerning the structure and properties of steels: simultaneous hardening, grain boundary and intragranular segregation of impurities (chiefly phosphorus). Therefore, it is useful to study separate contributions of these three phenomena to the slope. Moreover, the influence of hardening should be evaluated with the use of experimental data obtained for the steels which have undergone cold deformation.

As far as we know there are no experimental studies specially devoted to this problem, but the data from Refs. [52–61] show that cold deformation in steels can reduce the considered slope.

Experimental data obtained in studies of the development of temper embrittlement in steels show that in the cases where this phenomenon appears in an uncombined state, the transition curves are shifted upwards equidistantly from each other. Fig. 15 presents the change of the transition curve in steel 15Kh2MFA which had undergone temper embrittlement.

Experimental data obtained in the studies devoted to phosphorus segregation to interfaces (of precipitate/matrix type), i.e., intragranular segregation, show that in these cases the slope can diminish [66,74,75]. Most likely, the decrease in the level of the upper shelf observed in that

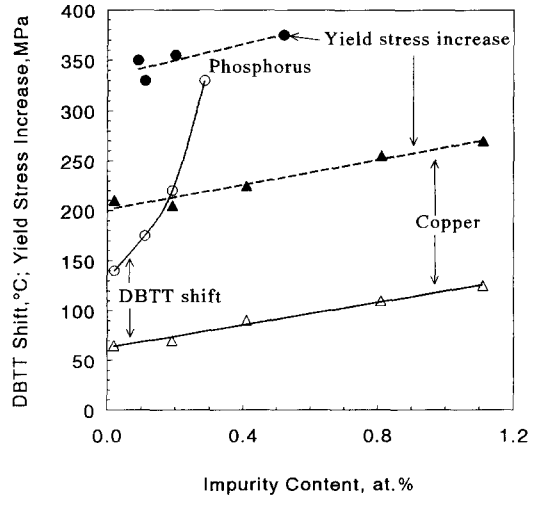

Fig. 14. Dependence of steel irradiation response on impurity content. $F = 4 \times 10^{23}$ n m^{-2}, irradiation temperature of 50°C [76].

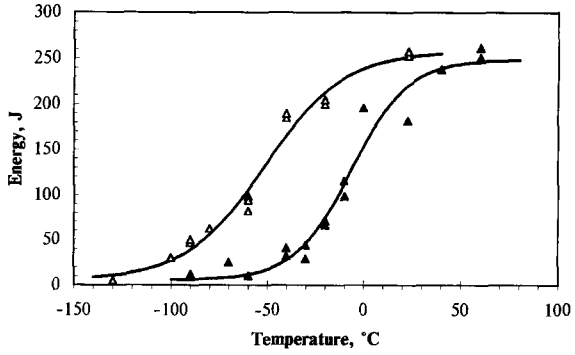

Fig. 15. Effect of temper embrittlement (thermal induced grain boundary segregation) on DBTT curve of 15Kh2NMFA type steel. (Δ) as-received condition; (▲) embrittled condition.

experiments is responsible for this phenomenon. It should be noted that usually any mechanisms responsible for the reduction of the slopes of the transition curves are not discussed in the current publications.

Probable reasons of the decrease in the level of the upper shelf in temperature dependencies of impact strength will be discussed in detail in Section 4.3, so now we summarize the results presented above.

The data described in this section indicate that if the phenomena of hardening and both grain boundary and intragranular phosphorus segregation in steels arise separately, then the reduction of the slope of the temperature dependence of the impact strength in the region of DBTT can occur only on account of hardening and intragranular phosphorus segregation.

4.3. Reduction of the upper shelf level in the transition curves

Now we consider the influence of cold deformation on USE. The number of experimental studies on this subject is quite insignificant [60–64]. Following Ref. [64], 4% cold deformation in steel produces the valuable shift in DBTT and actually does not change USE. In contrast, in Refs. [60–62] the reduction of USE resulting from cold deformation was registered. Quite different observations were made in Ref. [63]: with an increase in the degree of cold deformation occurring in RPVS A533B, when the monotone rise of the yield and ultimate stresses is observed, USE can either decrease or increase (Fig. 6). Using the considerations in Section 4.1, one can conclude that these peculiarities in the changes of USE can be evidently explained by specific properties of ductility in steels undergoing the corresponding degrees of cold deformation. Evidently the reduction of USE in steels resulting from cold deformation is caused only by the decrease in their ductility. But it is not improbable that at high degrees of cold deformation in steels the reduction of USE can be caused not only by the decrease in their ductility, but also by formation of voids. The latter process can produce the reduction of effective sections of the specimens and the corresponding reduction of USE.

Available publications on studies of reversible temper brittleness in steels show that grain boundary segregation of impurities (primarily phosphorus) do not produce the reduction of USE in the transition curves (even in the case of significant value of the upward shift in DBTT) (Fig. 15).

In a few available publications on the influence of intragranular phosphorus segregation it was demonstrated that their appearance in steels produces the reduction of USE in the transition curves [74,75]. This fact indicates the essential difference between grain boundary and intragranular phosphorus segregation emerging at the precipitate/matrix interfaces. These differences are clearly seen in the studies of fractures occurring in Charpy specimens which have undergone impact testing in the region of the upper shelf. The following fact is known from the studies on grain boundary phosphorus segregation: the fractures in specimens tested at the upper shelf temperatures do not contain areas with intragranular fracture (Table 2). This fact is true, although in testing of the same steels in the regions of the lower shelf and DBTT the fraction of the areas with intercrystalline fracture in specimen fracture surfaces may reach ~ 65–70%.

Noticeable phosphorus segregation at the precipitate/matrix interfaces in steels may be revealed in the fractures of the specimens tested in the region of the upper shelf. It is demonstrated in Refs. [74,75] that the boundaries of non-metallic inclusions, carbides of type M_6C and precipitates of Laves phases are the most typical locations of intragranular phosphorus segregation in A533B, A508 and some other Mn–Mo–Ni-steels. If the carbides or Laves phases decorate grain boundaries, then the areas with ductile intercrystalline fracture appear in fracture surfaces of specimens tested in the regions of the upper shelf and DBTT. A similar phenomenon has been observed by the authors of the present paper in irradiated steels of Russian and American grades and also in some cases after long-term thermal aging at the operating temperatures (Table 2, Figs. 12 and 13).

The above distinctions concerning the behaviour of grain boundary and intragranular phosphorus segregation, revealed in testing of specimens in the region of the upper shelf, are very important. They lead to the conclusion that in this temperature region the stress of tearing along intragranular segregation is essentially lower than the stress of tearing along grain boundary segregation. Besides, it means that in the region of the upper shelf the stress of tearing along phosphorus segregation at the interfaces is lower than the stress of tearing along the crystalline body. In testing with comparable temperatures the stress of tearing along grain boundary phosphorus segregation is higher than the stress of tearing along the crystalline body. The shortage of experimental data on phosphorus segregation

to interfaces in steels does not allow us to answer unambiguously the question about the reasons of reduction of the absorbed energy at the upper shelf due to emergence of the segregation. This reduction of the absorbed energy at the upper shelf could be explained by the decrease in steel ductility due to phosphorus segregation to interfaces (at deformation rates typical of impact testing). The reduction of the upper shelf can be also explained by the decrease in the effective specimen sections when phosphorus segregation is present at the precipitate/matrix interface. The last mentioned explanation might be the consequence of local decrease in stresses of tearing in the region of precipitate/matrix interface, where phosphorus segregation has appeared. Of course, both of the revealed reasons may contribute to the reduction of the upper shelf simultaneously. These peculiarities of phosphorus segregation to precipitate/matrix interface allow us to explain the rise of the upper shelf level to the value higher than initial one (i.e., in unirradiated steels) after annealing of irradiated RPVS that was observed in a few works (Fig. 16). One of the most probable explanations may be as follows. In some types of precipitate which exist in steel in the initial state and have propensity to phosphorus segregation, the heat treatment can produce this segregation to precipitate/matrix interface. Two processes due to irradiation may proceed in steels: the emergence of new locations for intragranular phosphorus segregation and the increase in phosphorus concentrations in existing segregation at the interfaces. These processes favour both the additional reduction of the level of the upper shelf and the DBTT shift. If the regimes of annealing applied to irradiated steels cause the decay of phosphorus segregation at interfaces of all precipitates which were present in steel initially (or the decrease in phosphorus concentrations in them to levels below initial), then the rise in USE might exceed the starting levels (in unirradiated state). Besides, these causes can lead to recovery of DBTT to temperatures lower than DBTT in unirradiated steels.

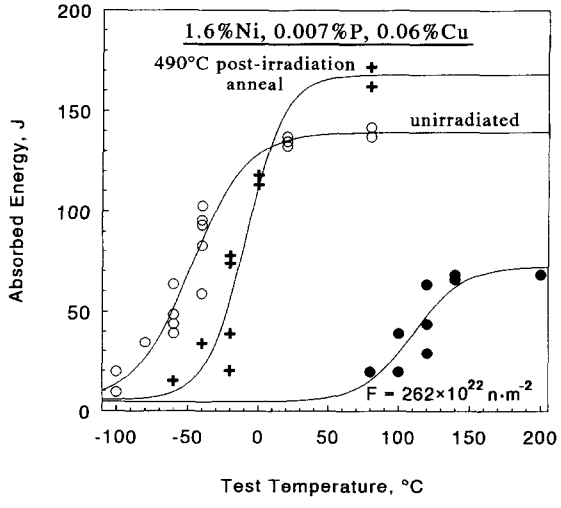

Fig. 16. Effect of post-irradiation annealing on transition curve.

Numerous published experimental data illustrate the influence of heat aging temperature on the rate of grain boundary phosphorus segregation in steels and also on temperature interval of their stability [66–68,71,72]. Only a few publications exist on phosphorus segregation to interfaces. Isolated experimental data deliver the evidence of the reversible character of phosphorus segregation to interfaces (i.e., the reversible character of intragranular phosphorus segregation) [74,75]. Some experimental data indicate that the temperatures of decay of intragranular phosphorus segregation are essentially lower than the temperatures of decay of grain boundary phosphorus segregation. The temperature of decay of grain boundary phosphorus segregation is usually ~ 600–650°C [66–68,71,72]. Alternatively, it is shown in Ref. [76] that the complete recovery of DBTT shift and USE in alloys Fe–P after irradiation at 50°C to neutron fluence $\sim 10^{23}$ n m^{-2} ($E > 0.5$ MeV) and subsequent annealing occurs at 420°C. In that study, absolutely convincing arguments were given that the shifts in DBTT and USE in alloys Fe–P are caused by intragranular phosphorus segregation.

The following fact engages our attention: the complete recovery of USE in RPVS of Russian and American grades irradiated at 250–290°C is observed after annealing at ~ 420°C [5,37,38,105].

The existing models of reversible temper brittleness assume the dependence of stability parameters and rates of phosphorus segregation on the structure and nature of the interfaces, where the segregation appears [65,78,79].

Summarizing the results of this section, the following conclusions can be drawn:

(i) the decrease in USE is connected with steel hardening in a complicated way. Steel hardening does not always induce the reduction of USE. Moreover, in some cases a rise might occur.

(ii) the accumulated experimental data demonstrate that two out of three of the above discussed mechanisms can induce the reduction of USE: hardening and intragranular phosphorus segregation.

5. Contribution to radiation embrittlement of pressure vessel steels from different mechanisms

In Section 4 three mechanisms were considered, combinations of which allow us to interpret the phenomena of RE in RPVS. The following scheme could be applied for a convincing experimental evaluation of their contributions to RE:

(i) Investigation of the dose dependencies of the DBTT shift and the reduction of the upper shelf. Study of influences of impurities and alloying elements (for instance, P, Cu, Ni, etc.) on the dependencies.

(ii) Investigation of the dose dependencies of both hardening and the change of steel ductility. Study of influences of impurities and alloying elements (for instance, P, Cu, Ni, etc.) on these dependencies.

(iii) Direct experimental study of the dose dependencies for the change of the RPVS phase composition: accumulation of radiation defects, copper-vacancy clusters and parameters of grain boundary and intragranular segregation. Study of influences of impurities and alloying elements (for instance, P, Cu, Ni, etc.) on these dependencies.

(iv) Investigation of recovery of the DBTT shift, USE, ductility and hardening in annealed irradiated RPVS.

(v) Direct experimental studies of influences of annealing on evolution of radiation-induced phases, defects, copper-vacancy clusters, grain boundary and intragranular impurity segregation, etc.

(vi) Inferences from items (i)–(v).

Nowadays such detailed and complete data on RE in RPVS are not available, therefore a reliable experimental assessment of the phenomena enumerated above is hampered. That is why the experimental data demonstrating separate influences of these three mechanisms on the transition curves are given in Sections 4.1, 4.2 and 4.3 and the data in Sections 5.1, 5.2 and 5.3 have to be analyzed.

5.1. The dose dependencies of the DBTT shift and change in yield stress for RPVS

It should be noted that only a few papers [5,22–33,105] were published which contain data on simultaneous measurements of the dose dependencies of the DBTT shift and yield stress carried out with RPVS specimens from the same melt. It should be noted as well that in the majority of the cases the dose dependencies for the DBTT shift and yield stress differ for Russian RPVS (both for base and weld metals) used in WWER-440 and WWER-1000. Fig. 17 shows the dose dependencies for the DBTT shift and $\Delta\sigma_{0.2}$ for these steels borrowed from [5,22,105]. It can be seen from Fig. 17a and b that in all cases the DBTT shift rises with an increase in neutron fluence. In contrast, dose dependencies for changes in the yield stress include regions of the yield stress decreasing with an increase in neutron fluence or the regions with the conserved values of $\Delta\sigma_{0.2}$. Thus, the discrepancy between the radiation-induced changes of yield stress and DBTT has been observed.

Some discrepancies are present in the dose dependencies for English RPVS (Fig. 18, Ref. [80]). The limited quantity of available experimental data does not allow us to justify qualitatively the influence of alloying elements and impurities in steels on the degree of the above discrepancies and the range of neutron fluences corresponding to the most significant discrepancies. The analysis of the available data has shown that as a rule the most valuable discrepancies in the dose dependencies for DBTT and $\sigma_{0.2}$ can be seen for the most important in practice neutron fluences of $\sim(1\text{–}5)\times 10^{23}$ n m^{-2} ($E > 0.5$ MeV).

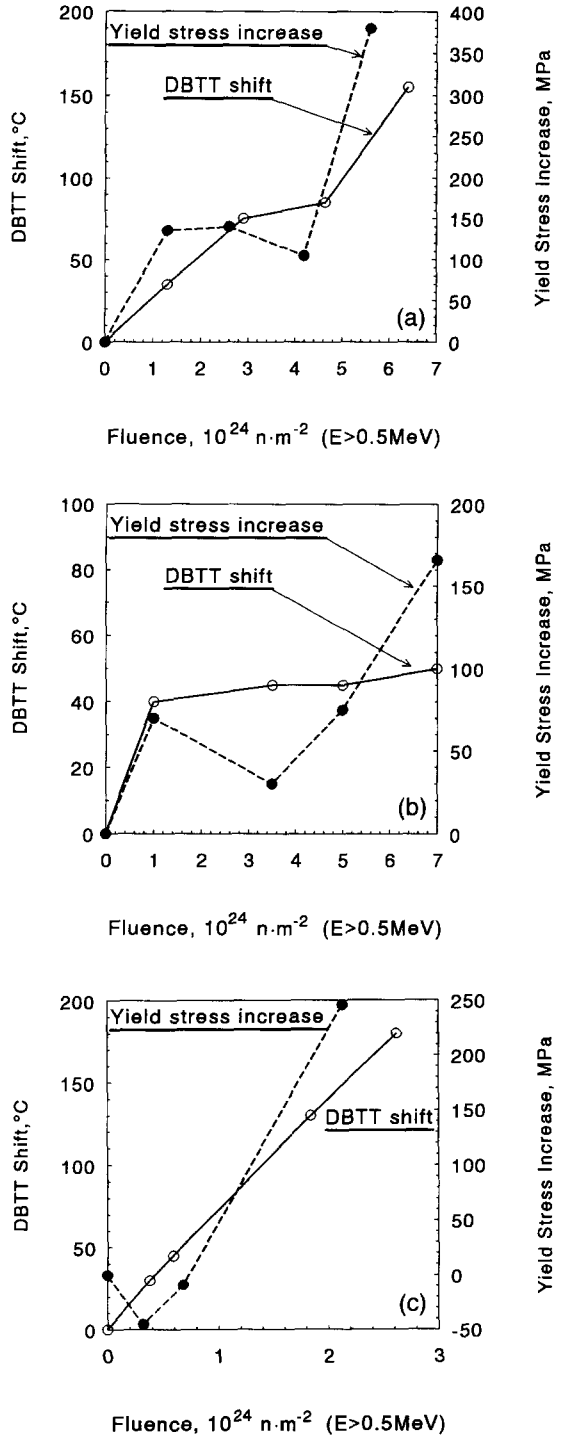

Fig. 17. Dependence of the DBTT shift and yield stress increase on neutron fluence for WWER-440 weld (a) and base metal (b) and for WWER-1000 weld (c) [5,22].

The existence of these discrepancies indicates the independence of some fraction of the DBTT shift produced by irradiation on hardening. This fact is most evident for the

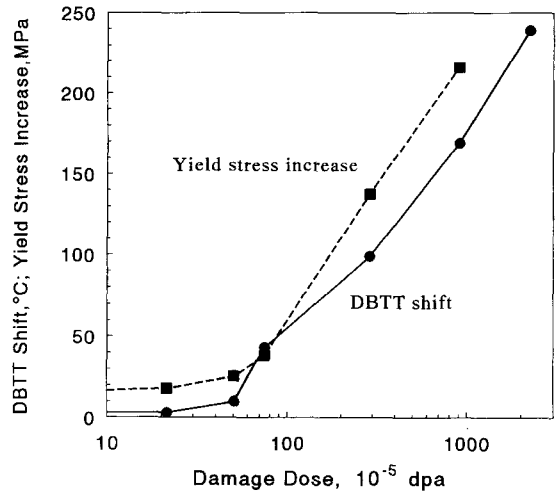

Fig. 18. Radiation response of UK-type steel [80].

range of neutron fluences corresponding to the increase in DBTT and simultaneous decrease or the absence of variations in $\sigma_{0.2}$ for RPVS with a rise in neutron fluence (Fig. 17).

It should be emphasized that the existence of the regions with the same behaviour in the dose dependencies for changes in the DBTT shift and $\sigma_{0.2}$ does not prove that the contribution from hardening into the change of DBTT for the corresponding neutron fluences is the decisive factor. To ascertain this is true, it is necessary to analyze the influence of impurity and alloy contents of the elements determining radiation-induced rise in DBTT on the change in yield stress resultant from irradiation. In addition, it is necessary to compare temperature dependencies of recovery of radiation-induced changes in DBTT and $\sigma_{0.2}$ due to annealing.

5.2. Dependence of radiation-induced changes in DBTT and $\sigma_{0.2}$ on concentrations of impurities and alloying elements.

The dependence of RE in steel 15Kh2NMFA on phosphorus content was studied in Ref. [32]. The phosphorus content in the steel varied from 0.005 to 0.035%. The specimens were irradiated at ~ 300°C to a fluence of $\sim 2 \times 10^{23}$ n m^{-2} ($E > 0.5$ MeV). It was shown that the coefficient of RE (A_F) increases linearly as a function of phosphorus concentration and its total increase is sevenfold in this range. On the other hand, the changes in the phosphorus concentration do not influence the changes in yield stress resulting from irradiation. Statistical processing of experimental data obtained in the testing of surveillance samples and other irradiated specimens made from steel 15Kh2NMFA and weld metal Sv.10KhGNMAA [81] has allowed the authors to reveal the influence of P and Cu impurities on the values of radiation-induced DBTT shift and A_F [81]. However, no notable influence of these impurities on the value of the change in $\sigma_{0.2}$ due to irradiation was revealed.

The investigation of phosphorus influence on radiation-induced changes in DBTT and $\sigma_{0.2}$ occurring WWER-440 steels irradiated at ~ 250–280°C showed that in some instances the increase in phosphorus content in steel causes changes in DBTT and $\sigma_{0.2}$ [81]. In contrast, statistical processing of a large body of experimental data obtained in [81] for irradiated surveillance samples and other specimens has not revealed any significant effect of P or Cu contents on changes in yield stress for WWER-440 RPVS materials. Similar statistical processing applied to the same data revealed the significant effect of P and Cu on the coefficient of RE [81] and, respectively, on the value of DBTT.

The radiation-induced increase in $\sigma_{0.2}$ in WWER-440 and WWER-1000 steels hampers an assessment of contribution from hardening to DBTT shift due to irradiation [105]. Primarily this is true for materials with the lowest content of the impurities. But for the materials demonstrating double and higher increase in the coefficient of RE (A_F) affected by increased P and Cu impurity content, it can be asserted that the contribution from hardening to radiation-induced DBTT shift is less than 50%. The latter assumption is absolutely true for WWER-440 RPVS applied in the first and second generations of NPP.

In a few works [1,35,82–86] devoted to investigation of influence of P and Cu on the changes in DBTT and $\sigma_{0.2}$ in RPVS of American grades the following was shown:

(i) An increase in Cu concentration reduces the phosphorus influence on RE (radiation-induced DBTT shift) in steel. For instance, in A533B with Cu content $< 0.01\%$, an increase in phosphorus concentration from 0.003 to 0.015% and 0.025% increased the radiation-induced DBTT shift (neutron fluence of $\sim 2.5 \times 10^{23}$ n m^{-2} ($E > 1$ MeV), irradiation temperature of 288°C) to 33 and 61°C, respectively. In contrast, when Cu content was 0.30%, the corresponding increase had constituted only 14 and 0°C, respectively. The change in radiation-induced DBTT shift in steel with phosphorus content of 0.003% due to the increase in Cu concentration from 0.002 to 0.3% was 136°C [82].

(ii) As a rule, the contribution from phosphorus to the radiation-induced DBTT shift is not associated with changes in $\sigma_{0.2}$ due to irradiation [83], but the influence of Cu on radiation-induced increase in yield stress is stated unambiguously [35,84–86].

5.3. Recovery of DBTT, $\sigma_{0.2}$ and the upper shelf level due to post-irradiation annealing

The analyses of numerous experimental data on RE in RPVS and some model materials points at the relations between the radiation-induced DBTT shift and the reduc-

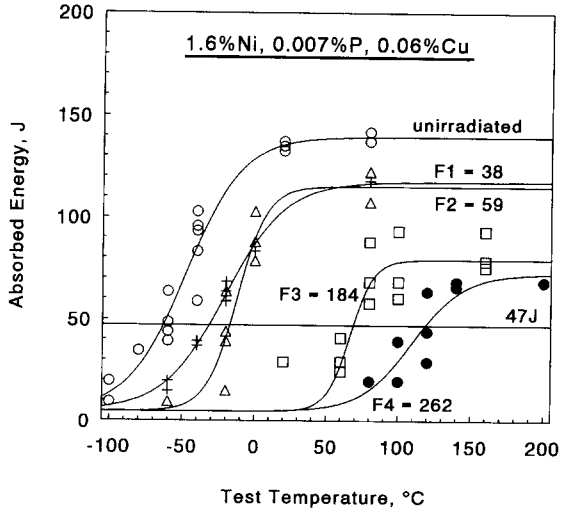

Fig. 19. Influence of irradiation on 15Kh2NMFA steel. $F_1 - F_4$ are fast neutron fluences in units 10^{22} n m^{-2}.

tion of USE. The same relations can be found in specimens made from steels irradiated to different neutron fluences either of the same (Fig. 19, from Ref. [5]) or different melts. The numerous experimental data presented in [87] demonstrate the proportionality between the reduction of USE due to irradiation and neutron fluence (Fig. 20) and, consequently, the DBTT shift. These facts are important for the analysis of the mechanisms determining RE in RPVS.

By now, the publications that include experimental studies of recovery of the DBTT shift, $\sigma_{0.2}$ and USE resulting from annealing of irradiated RPVS and some model materials (e.g., Refs. [1,5,88]) (Fig. 21) show the corresponding temperature dependencies of recovery for steels of Russian and American grades irradiated at operating temperatures. The large body of experimental data obtained in the studies of these types of steels [5,29,36,88–95,100] has been processed to obtain the curves. Some of the curves were presented in Refs. [5,88,90].

The analysis of the data in Fig. 21 shows that the following regularities are characteristic for irradiated steels of Russian and American grades after annealing:

(i) the temperature dependencies for the DBTT shift recovery are similar for the both types of RPVS. The recovery of the DBTT shift due to annealing at ~ 500°C exceeded ~ 80% in all the cases.

(ii) the temperature dependencies for USE recovery are similar for the both types of RPVS. In all the cases, actually complete recovery of the USE occurs already at annealing temperatures of ~ 420°C.

(iii) Ni, Cu and P reduce the degree of DBTT recovery resulting from annealing.

(iv) an increase in Ni content in steel leads to increase in the degree of recovery of the yield stress in compare with DBTT.

Noteworthy is that the temperatures of recovery of yield stress differ essentially for different types of RPVS. For instance, a complete recovery of irradiated RPVS 15Kh2NMFA occurs after annealing up to ~ 400°C (Fig. 21b). Under the same annealing conditions, the recovery of the DBTT shift is ~ 40% [5]. For irradiated steel 15Kh2MFA and the respective weld metal annealing at 400°C results in 60% recovery of the DBTT shift and 40% of $\sigma_{0.2}$ (Fig. 21, [88]).

Annealing of irradiated RPVS A302 at 400°C results in ~ 35% recovery of $\sigma_{0.2}$ and ~ 55% recovery of DBTT [29,89]. Annealing of irradiated RPVS A533B at 454°C results in ~ 90% recovery of $\sigma_{0.2}$ and ~ 65% recovery of DBTT [29,89]. The complete recovery of USE occurs for irradiated RPVS A533B after annealing at ~ 410–420°C and for steel A302 after annealing at ~ 400–410°C [89].

The experimental data displayed above show that the degree of recovery of the DBTT shift resulting from annealing of irradiated RPVS slightly correlates with the recovery of yield stress. Practically in all the cases the temperature of recovery of yield stress is either noticeably lower or noticeably higher than that for the DBTT shift (Fig. 21d and e). These and other experimental facts displayed here indicate that radiation hardening probably is not the factor determining the radiation-induced DBTT shift in RPVS.

The degree of recovery of the DBTT shift from ~ 50 to ~ 80% corresponds to annealing temperatures (400–420°C) providing complete recovery of USE practically in all steels. This peculiar feature indicates that the fraction of DBTT shift (RE) in RPVS, which is governed by the same mechanisms that govern the reduction of USE, is evidently responsible for major portion of RE.

Also noteworthy is that because of the slight correlation between the temperature of the complete recovery caused by annealing (at ~ 420°C) of the radiation-induced reduc-

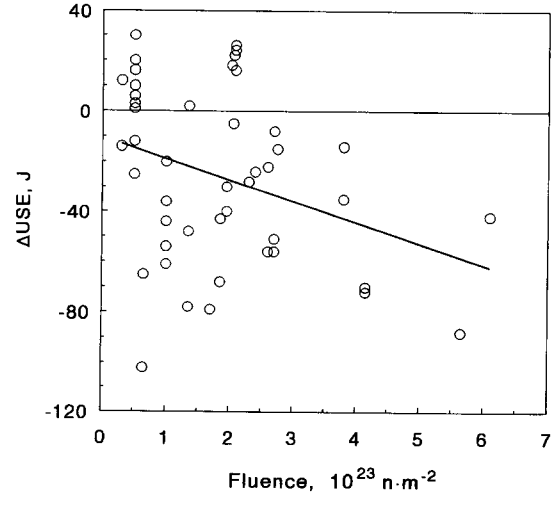

Fig. 20. Fluence dependence of USE decrease [87].

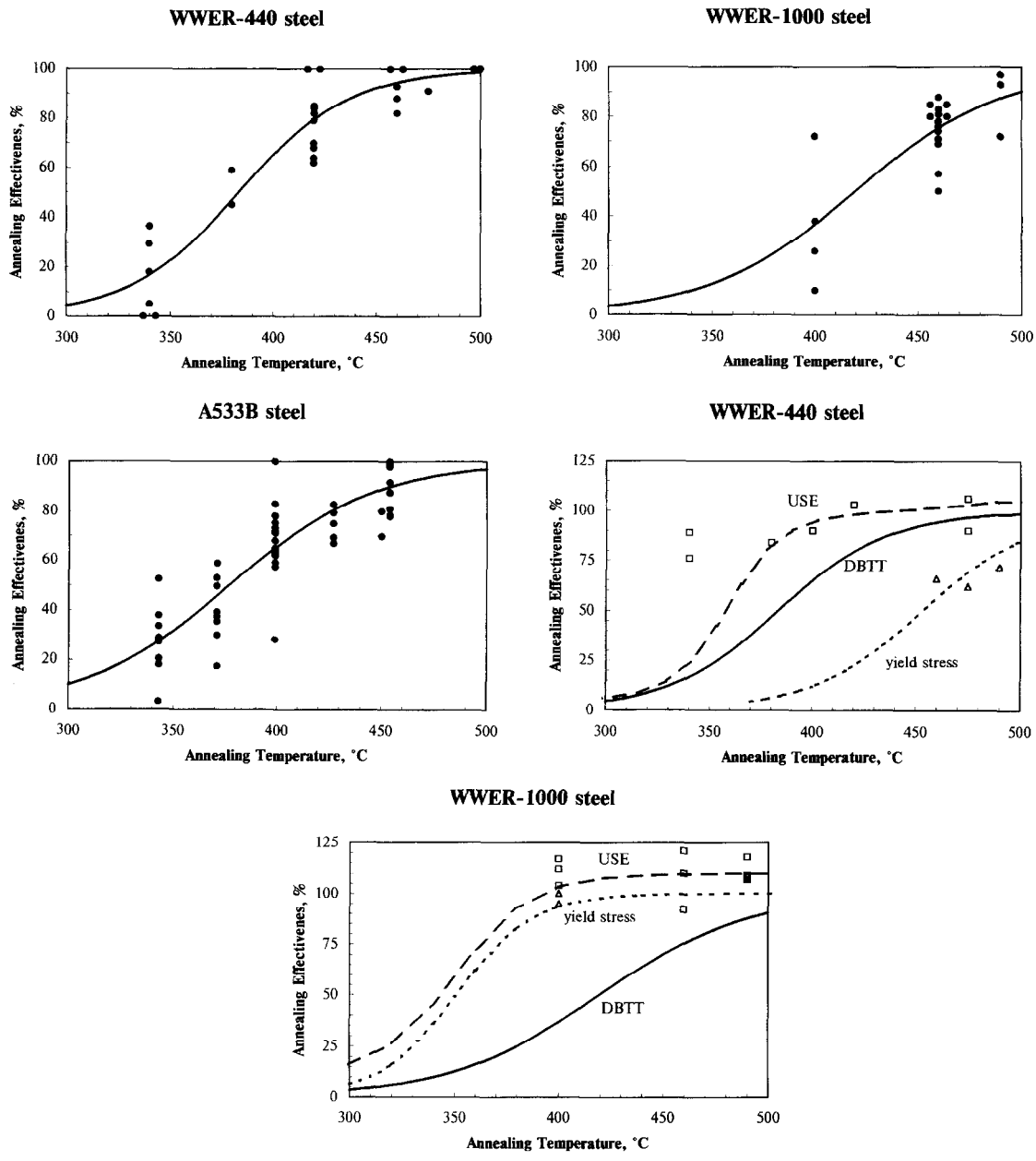

Fig. 21. The annealing effectiveness as a function of annealing temperature (for both weld and base metal). Annealing effectiveness = (1 − ⟨residual property change⟩/⟨radiation induced property change⟩) × 100% [5,29,36,88–95,100].

tion of USE in RPVS of Russian and American grades and the temperature of recovery of the corresponding changes in $\sigma_{0.2}$, the following conclusion can be deduced. Apparently, the radiation-induced reduction of USE in RPVS is determined to a considerable extent by the mechanisms independent on hardening in steels under irradiation.

In Sections 4.1, 4.2 and 4.3 the experimental data are displayed demonstrating that only two of three mechanisms of RE (which may in principle contribute to RE in RPVS) can cause the reduction of the upper shelf level. The third mechanism, i.e., grain boundary phosphorus segregation does not cause the reduction (Section 4.2). Therefore, the contribution from this segregation to the shift does not exceed 50% in steels of Russian and American grades.

Actually, this contribution is significantly lower. This fact becomes apparent if one assumes that the annealing temperatures required for decay of grain boundary phos-

phorus segregation are the same for segregation due to irradiation and thermal aging. The fractographic studies of irradiated and annealed RPVS (of Russian grades and some American) (Table 2) demonstrate that the above assumption is quite verisimilar. In all studied irradiated steels an annealing at 470–475°C either does not change the fraction of intercrystalline component in the fractures or induces its rise (Table 2). This means that annealing at these temperatures does not induce the decay of grain boundary phosphorus segregation present in irradiated steels. These convincing data testify that grain boundary phosphorus segregation due to irradiation are stable approximately at the same temperatures that are characteristic of segregation due to thermal aging. Hence it follows that in RPVS an annealing of that fraction of RE, which is determined by grain boundary phosphorus segregation, might begin at ≥ 470–500°C. If one takes account of temperature dependencies of recovery of the radiation-induced DBTT shift in annealed RPVS (see above), then the following can be deduced. Maximum contribution from grain boundary phosphorus segregation to RE (the DBTT shift) in RPVS does not exceed ~ 10–20%. This assertion is also supported by the data obtained for irradiated RPVS 25Kh3NM. In this steel irradiated at 270°C to ~ 1–5×10^{23} n m^{-2} ($E > 0.5$ MeV) the fraction of the regions with intercrystalline fracture in specimen fracture surfaces reached $\sim 70\%$ (Table 2). Nevertheless, the DBTT shift due to grain boundary phosphorus segregation has not exceeded $\sim 20\%$ of the total DBTT shift caused by irradiation.

Hence, the displayed results permit us to conclude that in RPVS of Russian and American grades the contribution of grain boundary phosphorus segregation to the radiation-induced DBTT shift (caused by irradiation to $< 10^{24}$ n m^{-2} at ~ 250–300°C) does not exceed ~ 10–20%. It is likely that just grain boundary phosphorus segregation in irradiated RPVS determines the fraction of the radiation-induced DBTT shift that is not recovered after annealing at ~ 450–500°C.

It was shown in Sections 4.1, 4.2 and 4.3 that the reduction of USE in transition curves obtained in impact testing can be caused by hardening and formation of intragranular phosphorus segregation in RPVS.

The data on the dose dependencies of the changes in DBTT, $\sigma_{0.2}$, phosphorus and copper influence on changes in DBTT and A_F and also the data on recovery of DBTT and $\sigma_{0.2}$ resulting from annealing of irradiated RPVS (Sections 5.1 and 5.2 and this section) indicate that at least in Russian RPVS with high content of P and Cu the hardening does not contribute the major portion to radiation-induced DBTT shift. The following experimental data support the proposition not only for Russian, but also for American grade steels:

(i) in the case of steel hardening due to cold deformation, even for the increase in $\sigma_{0.2}$ by the value significantly larger than hardening reached as a result of irradiation in RPVS, the DBTT shift does not exceed $\sim 50\%$ (Section 4.1). These values are much lower that the DBTT shifts observed in irradiated RPVS.

(ii) the shapes of dose dependencies of DBTT, temperature dependencies of both DBTT recovery and USE during annealing of irradiated RPVS of various types differ essentially slighter than the similar curves for $\sigma_{0.2}$.

6. Discussion of experimental data concerning the nature of radiation embrittlement in RPVS

In Section 4 it was indicated that the existing models and mechanisms of RE in RPVS have to explain at least qualitatively the whole complex of changes in the transition curves resulting from irradiation: the upward shift of the curve, the decrease in its slope in the region of DBTT and the decrease in USE.

The temperature dependence of yield stress specific for steels with BCC crystal lattice predetermines the appearance of brittleness in them at lowered temperatures (e.g., at the temperatures providing $\sigma_{0.2} = \sigma_b$). However, this temperature dependence of yield stress by itself does not explain the characteristic shape of the transition curve observed in impact testing. In Sections 4.1, 4.2 and 4.3, the assumption has been suggested that the transition curve is evidently determined by the character of the temperature dependence of ductility in these steels at deformation rates typical of impact testing (Fig. 7). Moreover, in Sections 4.1 and 4.2 the assumption has been suggested that both hardening in steels and formation of grain boundary or intragranular phosphorus segregation may produce upward shifts in temperature dependencies of ductility (at deformation rates typical of impact testing (Fig. 7). These shifts are apparently the direct cause of the shifts in the transition curves.

Actually, by now the experimental data on temperature dependence of ductility at high deformation rates typical of impact testing are absent. The above assumptions can be, in an indirect way, supported by the experimental data on lateral extension of specimens which have undergone impact testing. Clearly, due to the fact that the direct experimental evidence in not available, the development of reliable physical models of RE in steels (metals) is the subject of future studies. However, the analysis of different mechanisms aimed at their arrangement by their contribution to RE in RPVS remains instructive, as well as the attempts aimed at quality explanations (basing on the mechanisms) of the individual phenomena accompanying RE, for instance, the reduction of the upper shelf, are useful.

The considerations in Section 5 indicate that intragranular phosphorus segregation in RPVS resulting from irradiation can deliver the main contribution to radiation-induced rise in the DBTT shift and the reduction of the upper shelf. Nowadays, a rather limited number of publications exist involving considerations of the phenomena of the rise of

DBTT due to intragranular phosphorus segregation [74–76]. The assumption on the importance of the role of intragranular phosphorus segregation in RE occurring in some RPVS was suggested rather long ago [32]. But in the literature the problem of the influence of intragranular phosphorus segregation on the whole complex of RE phenomena in RPVS was not even posed.

The reasons that may be responsible for the reduction of USE of the temperature dependencies of impact strength due to intragranular phosphorus segregation are discussed in Section 4.3. The most important factors in this reduction are probably the low levels of tearing stress and ductility in those microvolumes of the material where intragranular phosphorus segregation are located.

The value of relative reduction of USE (ΔUSE/USE) caused by intragranular phosphorus segregation can be evaluated as follows. A_1 denotes the specific absorbed energy in the steel (i.e., the absorbed energy divided by the unit area of the operating section of a specimen) at the upper shelf assuming that intragranular phosphorus segregation does not occur. Respectively, A_2 is the specific absorbed energy within the region where intragranular phosphorus segregation has occurred, $A_2 < A_1$. Then

$$\mathrm{USE} = A_1 S, \tag{16}$$

where USE is the steel absorbed energy at the upper shelf prior to intragranular phosphorus segregation and S the operating section of the specimen.

Similarly, the value of change in the absorbed energy (ΔUSE) induced by intragranular phosphorus segregation may be represented in the following way:

$$\Delta\mathrm{USE} = A_1 S - \left[A_1(S - \Delta S) + A_2 \Delta S \right] = (A_1 - A_2)\Delta S, \tag{17}$$

where ΔS is the total area of the regions on the operating section of a specimen where intragranular phosphorus segregation is located. Then

$$\frac{\Delta\mathrm{USE}}{\mathrm{USE}} = \frac{(A_1 - A_2)}{A_1}\frac{\Delta S}{S}. \tag{18}$$

In the general case $A_2 = f(C_\mathrm{P})$, i.e., A_2 is a function of phosphorus concentration (C_P) in intragranular segregation. Consequently,

$$\frac{\Delta\mathrm{USE}}{\mathrm{USE}} = \left(1 - \frac{f(C_\mathrm{P})}{A_1}\right)\frac{\Delta S}{S} = F(C_\mathrm{P})\frac{\Delta S}{S}, \tag{19}$$

where $F(C_\mathrm{P}) = 1 - f(C_\mathrm{P})$. The function $F(C_\mathrm{P})$ increases with the rise in phosphorus concentration. At high concentrations, if one assumes $A_2 \ll A_1$, then $F(C_P) \approx 1$ and

$$\Delta\mathrm{USE}/\mathrm{USE} = \Delta S/S. \tag{20}$$

The essential distinction of intragranular segregation compared to grain boundary segregation is that they do not form continuous spatial surfaces inside the volume of the material. For this reason, the degree of influence of intragranular segregation on the absorbed energy depends not only on phosphorus concentrations in them, but both on the average size of precipitate (to the interfaces of which phosphorus segregates) and the average distance between them. For example, in the simplest case of spherical inclusions of radius r, forming 3D regular cubic lattice of period R, it can be shown that if the operating section is one of the planes of this lattice, then the quantity n of inclusions inside the section of area S is

$$n = S/R^2. \tag{21}$$

Respectively, the area of the operating section occupied by precipitate (to the interfaces of which phosphorus has segregated) ΔS is equal to

$$\Delta S = n\pi r^2 = S\pi r^2/R^2. \tag{22}$$

Therefore, the value of $\Delta S/S$ in Eqs. (18) and (19) is equal to

$$\Delta S/S = \pi r^2/R^2. \tag{23}$$

in the case considered. If N denotes the value of the volume density of the precipitate, then $N = 1/R^3$ and thus

$$\Delta S/S = \pi r^2 N^{2/3}. \tag{24}$$

In the more general case, when the precipitate has randomly distributed locations inside the volume of material with the average radius $\langle r \rangle$, average distance $\langle R \rangle$ and volume density N, then

$$\Delta S/S \sim \langle r \rangle^2/\langle R \rangle^2 \sim \langle r \rangle^2 N^{2/3}. \tag{25}$$

Taking into account the relationship $(A_1 - A_2)/A_1 = F(C_\mathrm{P}) < 1$ and Eq. (20), one can see that the ratio ΔUSE/USE is always larger than the similar value calculated with the use of Eq. (19). So, using Eq. (20), one can obtain the upper boundary for the influence of intragranular phosphorus segregation on the relative change in USE.

In particular cases, the precipitate that has phosphorus segregation at its interfaces may be situated at grain boundaries. If their density is high enough in the fractures of Charpy specimens tested within the regions of DBTT and the upper shelf, then the regions with ductile intercrystalline fractures may appear (Table 2 and Fig. 13) [74,75]. This situation, when precipitates with phosphorus segregation at its interfaces are located both inside the volume and at grain boundaries, is quite realistic [74,75].

The evolution of intragranular phosphorus segregation in steels induced by thermal aging may be attributed to a few processes:

(i) the changes in phosphorus concentrations in the interfaces of the precipitates.

(ii) the changes in the phase composition of the steel accompanied by formation of new precipitates with phosphorus segregation to their interfaces.

(iii) simultaneous occurrence of the processes from items (i)–(ii).

In the case of irradiation the following items are added to items (i)–(iii):

(iv) phosphorus segregation to radiation defects.

(v) phosphorus segregation to radiation-induced inclusions and clusters of various types, for instance, copper-vacancy clusters etc.

In recent years a valuable quantity of publications appeared containing data on the formation of various types of clusters and precipitates in irradiated RPVS in addition to radiation defects (dislocation loops). For example, in Refs. [4,27], the copper-vacancy clusters and also other types of precipitates have been observed in irradiated RPVS. In some instances the presence of phosphorus was revealed in the precipitate observed. Usually, the sizes of the clusters and inclusions do not exceed ~ 1–10 nm. Any direct experimental registration of these or determination of their chemical composition is a rather difficult problem. That is why the presence or absence of phosphorus segregation at the clusters, precipitate or radiation defects is not reliably established.

Nevertheless, it is well-known that phosphorus is one of the elements present in the steels in solid solution and is involved in interaction with fluxes of point defects resulting from microstructure gradients during irradiation. This mechanism (solute drag) leads to impurity segregation (e.g., phosphorus) to various types of sinks in steels during irradiation [101]. This mechanism can be realized at significantly lower temperatures than necessary for phosphorus segregation during aging.

Likewise, the above considerations and Eqs. (20) and (24) permit us to assess the probable contribution of radiation-induced phosphorus segregation to interfaces to the reduction of USE in irradiated RPVS of various grades.

In accordance with Refs. [4,27,69], in RPVS of American grades, under real operating conditions, the dominating type of structural changes is formation of precipitates enriched with Cu. Under irradiation, their density and radius may reach $\sim 2 \times 10^{19}$ cm^{-3} and ~ 1–2 nm, respectively. In the case of phosphorus segregation at the interfaces of the Cu precipitate/matrix the value of reduction of USE due to this segregation can be derived using Eqs. (20) and (24):

$$(\Delta \mathrm{USE}/\mathrm{USE}) \times 100\% \approx (\Delta S/S) \times 100\% \approx 15\%. \tag{26}$$

This value is in good agreement with relative changes in USE due to irradiation of these steels in the corresponding conditions. The latter fact is of importance since an appearance of precipitate enriched with Cu due to irradiation, which causes radiation strengthening, does not explain by itself the value of the radiation-induced reduction of USE.

The electron-microscope studies of Russian RPVS performed by the authors show that in realistic irradiation conditions, in addition to radiation defects (dislocation loops), exist disk-shaped inclusions ~ 1 nm thick and ~ 10 nm in diameter. Table 3 presents the data on densities and sizes of the radiation defects and disk-shaped inclusions for Novovoronezh NPP-2 weld metal in various states. The front- and sideview of disk-shaped inclusions are shown in Fig. 22. These inclusions lie at the crystallographic planes of the type {100}. If one assumes that phosphorus segregates to the interface of the disk-shaped inclusions, then the approximate evaluation of the relative reduction of the upper shelf (for precipitate of density $\sim 7 \times 10^{16}$ cm^{-3}, ~ 5 nm radius) is: $(\Delta \mathrm{USE}/\mathrm{USE}) \times 100\% \approx 10\%$. This value of $\Delta \mathrm{USE}/\mathrm{USE}$ is in agreement with experimental values of reduction of USE due to irradiation.

It would be interesting to study the behaviour of phosphorus segregation to interfaces during annealing. This behaviour could significantly elucidate the peculiarities of recovery of the properties in irradiated RPVS.

The temperatures providing annealing of phosphorus segregation at the interface (in contrast with grain boundary phosphorus segregation) may be defined by the following two processes:

(i) dissolution and transfer to the matrix of phosphorus that segregates to interfaces.

(ii) dissolution of the precipitate containing phosphorus

Table 3
Density and dimensions of radiation defects and disk-shaped precipitates in weld metal of NVNPP-2 pressure vessel

Layer	Conditions	n_{loops} ($\times 10^{15}$ cm^{-3})	d_{loops} (nm)	n_{disk} ($\times 10^{15}$ cm^{-3})	d_{disk} (nm)
Inner (8)	irradiated to $F = 6.5 \times 10^{19}$ n cm^{-2}	7–8	5	50–60	10.5
Inner (8)	irrad. + anneal. 475°C/150 h	–	–	3.5–4.0	13.5
Inner (8)	irrad. + anneal. 560°C/2 h	–	–	0.7–0.9	20.5
Extern (1)	irradiated to $F = 2.4 \times 10^{19}$ n cm^{-2}	5–6	3	30–50	9.5
Extern (1)	irrad. + anneal. 475°C/150 h	–	–	2.5–3.0	17.5
Extern (1)	irrad. + anneal. 560°C/2 h	–	–	0.9–1.0	23.5
	unirradiated	–	–	0.5–0.6	20.4

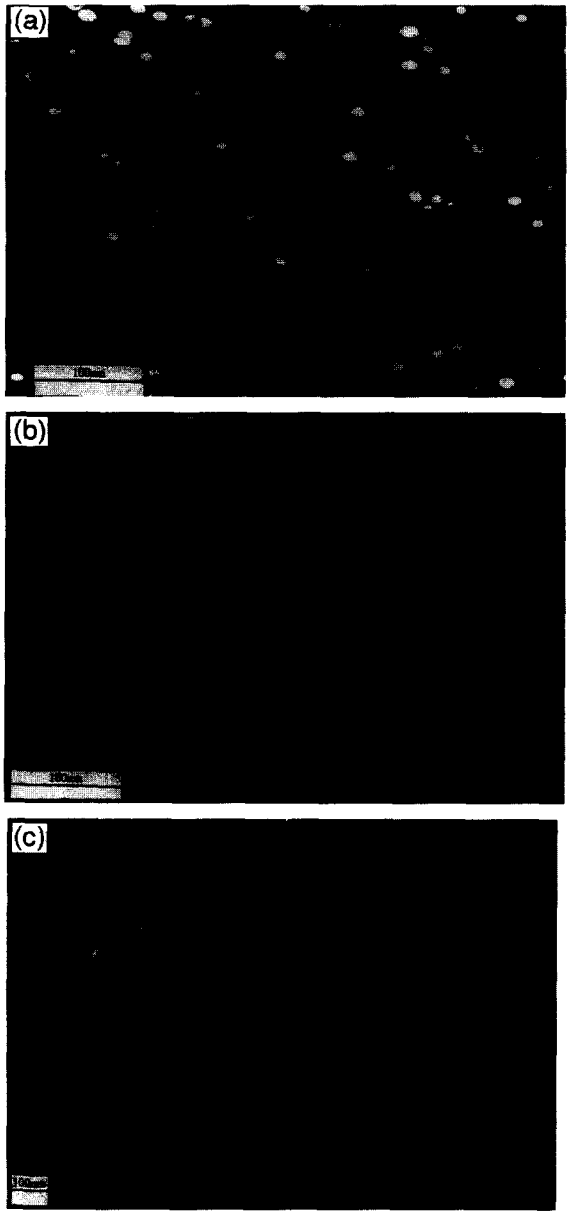

Fig. 22. Disk-shape precipitates in the irradiated weld metal (WWER-440 trepan). (a) front view; (b) side view and (c) precipitates decorated grain boundaries.

at its interfaces and subsequent disappearance of the phosphorus segregation.

Minimum annealing temperature necessary for disappearance of phosphorus segregation at the interfaces is determined by the minimum temperature sufficient for realization of one of the processes: (i) or (ii). This circumstance distinguishes phosphorus segregation at interfaces from that at grain boundaries. In the latter, disappearance of phosphorus segregation during annealing (at < 700°C) is possible only for its dissolution and transfer from grain boundaries to the matrix.

It is well known that formation and behaviour of grain boundary phosphorus segregation in steels during thermal aging can be described using the thermodynamic state functions [96]. For this reason, the concentration of phosphorus in grain boundary segregation is independent on the previous history of the material (i.e., on keeping of the steel at temperatures < 700°C). It has been demonstrated above that the experimental data exist, demonstrating that this is valid also for grain boundary phosphorus segregation due to irradiation. Thus, phosphorus concentration in grain boundary segregation depends only on annealing temperature, if the duration of annealing is long enough. Besides, the concentration may depend on the rate of cooling after annealing.

Nowadays there exists a rather limited quantity of experimental data on formation and behaviour of phosphorus segregation at interfaces at thermal aging of steels [74,75]. These data points to the fact that apparently these processes may be described with the use of the thermodynamic state functions too. Evidently, it might be assumed that in this case phosphorus concentration in interface segregation also depends only on annealing temperature for a long enough duration of annealing.

The temperatures of the most active formation and decay of phosphorus segregation on interfaces may depend on the types of these precipitates. The data from Refs. [74,75] indicate that these temperatures in the RPVS examined at thermal aging are likely to be some lower than the corresponding temperatures for grain boundary phosphorus segregation. But the difference evidently is not significant enough to predict dissolution of phosphorus segregation in the matrix at annealing temperatures $\lesssim 400$–420°C.

Compare the kinetics of the enrichment of intercrystalline and precipitate/matrix interfaces at temperature, T. After quick cooling from the temperature of high temper, grain boundary phosphorus concentration changes in compliance with the following regularity [68,96,106]:

$$C_{\mathrm{P}}^{\mathrm{GB}}(t) = C_{\mathrm{P}\infty}^{\mathrm{GB}} - \left(C_{\mathrm{P}\infty}^{\mathrm{GB}} - C_{\mathrm{P}0}^{\mathrm{GB}}\right)\exp\left[\omega^2(t)\right]\mathrm{erfc}\left[\omega(t)\right]. \tag{27}$$

Here t designates the time period of aging at temperature T.

$$C_{\mathrm{P}0}^{\mathrm{GB}} = C_{\mathrm{P}}^{\mathrm{GB}}(t=0), \qquad C_{\mathrm{P}\infty}^{\mathrm{GB}} = C_{\mathrm{P}}^{\mathrm{GB}}(t\to\infty)$$

$$\mathrm{erfc}(\omega) = 1 - \mathrm{erf}(\omega) = \frac{2}{\sqrt{\pi}}\int_{\omega}^{\infty}\exp(-x^2)\,\mathrm{d}x;$$

$$\omega(t) = 2\sqrt{D_{\mathrm{P}}t}\,/\eta h,$$

where $\eta = C_{\mathrm{P}\infty}^{\mathrm{GB}}/C_{\mathrm{P}}^{0}$; h is the thickness of adsorbing region; C_{P}^{0} is the bulk phosphorus concentration in the steel; D_{P} is the phosphorus diffusivity.

In Ref. [104] the following equation for thermodynamic

equilibrium phosphorus concentration $C_{P\infty}^{GB}$ was suggested for RPVS of WWER grade:

$$C_{P\infty}^{GB} = C_P^0 \exp(\Delta G_P/kT)/\{1 + C_P^0(\exp(\Delta G_P/kT) - 1)\}. \quad (28)$$

where ΔG_P is the heat of phosphorus adsorption at grain-boundaries. Taking into account the strong influence of Ni on grain-boundary phosphorus segregation [11,68], one defines ΔG_P as follows:

$$\Delta G_P = \Delta G_P^0 + \gamma_{Ni-P} C_{Ni\infty}^{GB};$$

$$\Delta G_{Ni} = \Delta G_{Ni}^0 + \gamma_{Ni-P} C_{P\infty}^{GB}. \quad (29)$$

Here ΔG_P^0 is the heat of grain boundary adsorption in Ni-free α-Fe. The equilibrium grain boundary Ni concentration $C_{Ni\infty}^{GB}$ is defined by the relations similar to Eqs. (28) and (29) for calculation of $C_{P\infty}^{GB}$. The values below have been chosen in Ref. [68] as the model parameters:

$$\Delta G_P^0 = 0.43 \text{ eV}, \qquad \Delta G_{Ni}^0 = 0.12 \text{ eV},$$

$$\gamma_{Ni-P} = 0.31 \text{ eV}, \qquad h = 0.33 \text{ nm}.$$

$$D_P = D_0 \exp(-Q/kT), \qquad D_0 = 7.12 \times 10^{-3} \text{ m}^2/\text{s},$$

$$Q = 258 \text{ kJ/mol}.$$

Solving the diffusion equation

$$\frac{\partial C}{\partial t} = D\frac{\partial^2 C}{\partial \rho^2} + \frac{2}{\rho} D\frac{\partial C}{\partial \rho} \quad (30)$$

with the use of the Laplace transform, one may obtain an expression describing the kinetics of phosphorus segregation to the surface of small spherical inclusion of radius, ρ_0 [70]. In notations of Eqs. (27) and (28) the solution has the form

$$C_P^G(t) = C_{P\infty}^G - (C_{P\infty}^G - C_{P0}^G) \times \exp[-at] \times \left\{ \exp(i\rho_0\sqrt{a})\operatorname{erf}\left(\frac{\rho_0 + 2i\sqrt{at}}{2\sqrt{t}}\right) - \exp(-i\rho_0\sqrt{a})\operatorname{erf}\left(\frac{-\rho_0 + 2i\sqrt{at}}{2\sqrt{t}}\right)\right\}/2, \quad (31)$$

where $a = D/\eta h \rho_0$. The bonding energy between phosphorus atoms and the precipitate has been chosen in compliance with Ref. [107].

The analysis of Eq. (31) shows that the rate of phosphorus adsorption to precipitate exceeds the rate of grain boundary adsorption.

It was pointed out above that the disappearance of phosphorus segregation at interfaces (or surfaces of radiation defects) during annealing (in contrast with grain boundary phosphorus segregation) may also be attributed to the disappearance of the corresponding precipitate (radiation defects) in the matrix.

The data obtained in the electron-microscope studies presented in Table 3 show that an annealing at 475°C produces complete disappearance of radiation defects (dislocation loops) and reduction of density of disk-shaped inclusions approximately fourteen times. Annealing at 560°C reduces the density of those inclusions actually to initial values (in unirradiated material). The data indicate that disappearance of phosphorus segregation at interfaces resulting from annealing in irradiated RPVS of Russian grades can be quite satisfactory explained by dissolution of the corresponding precipitate (radiation defects) in the matrix.

The available experimental data indicate that annealing of American grade steels at ~ 470°C produces dissolution of valuable fraction of the radiation-induced Cu-enriched precipitate [35]. It can be predicted that the annealing inducing dissolution of precipitate in the matrix would cause also disappearance of the phosphorus segregation in the locations of interfaces of already dissolved precipitate, if phosphorus segregation was present at the surface of this precipitate.

The results and considerations displayed above allow us to conclude that minimum values of the temperature sufficient for the annealing of phosphorus segregation at interfaces in irradiated RPVS might be determined by the temperatures of dissolution in the matrix of the corresponding precipitate, but not by the temperatures of dissolution of the phosphorus segregation itself.

It should be emphasized that phosphorus segregation to interfaces may appear in RPVS already in the initial state (unirradiated). It may occur during cooling after steel tempering (at 620–700°C). Formation of interfacial segregation due to steel cooling after tempering is more probable than grain boundary phosphorus segregation. The reason is that the temperatures of the most active phosphorus segregation to interfaces are evidently some lower than that ones for grain boundary phosphorus segregation. The irradiation of steel results in further development of phosphorus segregation to interface inclusions which were present in unirradiated material and also to the formation of such segregations at the emerging radiation-induced precipitate. Subsequent recovery annealing of RPVS irradiated at ~ 500–650°C may cause complete dissolution of phosphorus segregation at the inclusions which were present in unirradiated steel (and also on the radiation-induced precipitate in accordance with the mechanism described above). If the cooling conditions of irradiated RPVS after annealing at ~ 500–650°C do not produce phosphorus segregation to interfaces, then the recovery of the DBTT shift may exceed 100%. Moreover, in this case, USE may exceed the corresponding value for unirradiated steels.

7. Conclusion

The analysis of data from the literature on radiation embrittlement in pressure vessel steels and also the results obtained by the authors demonstrate the following.

(1) The sum total of phenomena due to radiation embrittlement in pressure vessel steels is determined by the cooperative action of three mechanisms: matrix radiation hardening, grain boundary segregation of impurities and segregation of impurities to precipitate interfaces.

(2) An essential part of radiation embrittlement in pressure vessel steels can be attributed to phosphorus segregation to interfaces induced by irradiation.

(3) Grain boundary phosphorus segregation in irradiated pressure vessel steels is responsible for an insignificant portion of the radiation-induced DBTT shift, not exceeding ~ 10–20%.

Noteworthy is that the available experimental data are absolutely insufficient for the development of a detailed understanding of the nature of radiation embrittlement in pressure vessel steels and further investigations are needed.

Acknowledgements

The present work has been carried out at the Reactor Materials Division of Russian Research Center 'Kurchatov Institute'. The authors are thankful to their colleagues from the Department: P.A. Platonov, E.A. Krasikov, A.D. Amaev, A.M. Kryukov, O.V. Lavrenchuk, V.N. Nevzorov, Yu.N. Korolev, Yu.R. Kevorkyan, O.O. Zabusov and K.E. Prikhod'ko for useful discussions and help.

References

[1] J.R. Hawthorne, in: Treatise on Materials Science and Technology, eds. C.L. Briant and S.K. Bunerji, Vol. 25 (Academic Press, New York, 1983) ch. 10.
[2] L'. Kupca, Š. Cepcek, in: Radiation Embrittlement of Nuclear Reactor Pressure Vessel Steels, ASTM STP 1170, ed. L.E. Steele (American Society for Testing and Materials, Philadelphia, PA, 1993) p. 380.
[3] G.R. Odette, G.E. Lucas, in: Radiation Embrittlement of Nuclear Reactor Pressure Vessel Steels, ASTM STP 909, ed. L.E. Steel (American Society for Testing and Materials, Philadelphia, PA, 1986) p. 206.
[4] M.K. Miller, M.G. Burke, J. Nucl. Mater. 195 (1992) 68.
[5] Yu.A. Nikolaev, A.V. Nikolaeva, A.M. Kryukov, V.I. Levit, Yu.N. Korolev, J. Nucl. Mater. 226 (1995) 144.
[6] J.R. Hawthorne, Nucl. Technol. 59 (1982) 440.
[7] M.G. Burke, M.K. Miller, J. Phys. (Paris) 49-C6 (1988) 283.
[8] G. Brauer, F. Eichhorn, Nucl. Eng. Design 143 (1993) 301.
[9] F.V. Nolfi, ed., Phase Transformations During Irradiation (Applied Science, London, 1983).
[10] M.K. Miller, R. Jayaram, K.F. Russell, J. Nucl. Mater. 225 (1995) 215.
[11] Yu.A. Nikolaev, A.V. Nikolaeva, O.O. Zubusov, B.A. Gurovich, E.A. Kuleshova, A.A. Chernobaeva, Fiz. Metall. Metalloved. 81-1 (1996).
[12] M.K. Miller, M.G. Burke, J. Phys. (Paris) 48-C6 (1987) 429.
[13] M.K. Miller, M.G. Burke, in: Proc. 3rd Int. Symp. on Environmental Degradation in Nuclear Power Systems, Water Reactors, eds. J.T.A. Robert, J.R. Weeks and G.J. Theus (The Metallurgical Society of AIME, Warrendale, PA, 1988) p. 141.
[14] S.G. Druce, in: Effects of Radiation on Materials, ASTM STP 1046, eds. N.H. Packan, R.E. Stoller and A.S. Kumar (American Society for Testing and Materials, Philadelphia, PA, 1990) p. 30.
[15] A.V. Nikolaeva, Yu.A. Nikolaev, A.M. Kryukov, J. Nucl. Mater. 218 (1994) 85.
[16] B.A. Gurovich, A.I. Ryazanov, L.A. Elesin, I.A. Altovsky, P.A. Platonov, ASTM STP 570 (1976) 599.
[17] U.S. NRC Regulatory Guide 1.99, Rev. 1, 1977.
[18] U.S. NRC Regulatory Guide 1.99, Rev. 2, 1988.
[19] Calculation Standards for Strength of Equipment and Pipes of Nuclear Power Units, PNAE-G-7-002-86, Erergoatomizdat, Moscow, 1989.
[20] L.S. Zazhigaev, A.A. Kushyan, Yu.I. Romanikov, Methods of Planning and Treatment om Physical Experiment Results (Atomizdat, Moscow, 1978).
[21] F.M. Haggay, in: Effects of Radiation on Materials, ASTM STP 1175, eds. A.S. Kumar, D.S. Gelles, R.K. Nanstad and E.A. Little (American Society for Testing and Materials, Philadelphia, PA, 1993) p. 172.
[22] A.D. Amaev, A.M. Kryukov, V.I. Levit, M.A. Sokolov, in: Radiation Embrittlement of Nuclear Reactor Pressure Vessel Steels, ASTM STP 1170, ed. L.E. Steele (American Society for Testing and Materials, Philadelphia, PA, 1993) p. 9.
[23] R.L. Simons, in: Influence of Radiation on Material Properties, ASTM STP 956, eds. F.A. Garner, C.H. Henager and N. Igata (American Society for Testing and Materials, Philadelphia, PA, 1987) p. 535.
[24] R.W.K. Honeycombe, The Plastic Deformation of Metals (Edward Arnold, 1968).
[25] F.A. Garner, in: Material Science and Technology: A Comprehensive Treatment, Vol. 10A, Nuclear materials, Part 1, ed. B.R.T. Frost (VCH, Weinheim, 1994) ch. 6.
[26] V.G. Kapinos, P.A. Platonov, Radiat. Eff. 103 (1987) 45.
[27] G.R. Odette, Scripta Metall. 17 (1983) 1183.
[28] G.R. Odette, P.M. Lombrazo, R.A. Wullaert, Effects of Radiation on Materials, ASTM STP 870 (American Society for Testing and Materials, Philadelphia, PA, 1985) p. 840.
[29] J.R. Hawthorne, in: Effects of Radiation on Materials, ASTM STP 782, eds. H.R. Brager and J.S. Perrin (American Society for Testing and Materials, Philadelphia, PA, 1982) p. 375.
[30] C. Guionnet, Y. Robin, C. Flavier et al., in: Effects of Radiation on Materials, ASTM STP 728, eds. D. Kramer, H.R. Brager and J.S. Perrin (American Society for Testing and Materials, Philadelphia, PA, 1981) p. 20.
[31] C. Guionnet, B. Houssin, D. Brasseur et al., in: Effects of Radiation on Materials, ASTM STP 782, eds. D. Kramer, H.R. Brager, J.S. Perrin (American Society for Testing and Materials, Philadelphia, PA, 1982) p. 392.

[32] N.N. Alexeyenko, A.D. Amaev, I.V. Gorynin, V.A. Nikolaev, Iradiation Damage of Pressured Water Reactor Vessel Steels (Energatomisdat, Moscow, 1981).
[33] T. Páv, J. Kocik , E. Keilová, in: Radiation Embrittlement of Nuclear Reactor Pressure Vessel Steels, ASTM STP 1170, ed. L.E. Steele (American Society for Testing and Materials, Philadelphia, PA, 1993) p. 300.
[34] R.K. Nanstad, R.G. Berggren, in: Effects of Radiation on Materials, ASTM STP 1175, eds. A.S. Kumar, D.S. Gelles, R.K. Nanstad, E.A. Little (American Society for Testing and Materials, Philadelphia, PA, 1993) p. 239.
[35] G.R. Odette, G.E. Lucas, D. Klingensmith, in: Effects of Radiation on Materials: 17th Int. Symp., ASTM STP 1270, eds. D.S. Gelles, R.K. Nanstad, A.S. Kumar and E.A. Little (American Society for Testing and Materials, Philadelphia, PA, 1994).
[36] G.R. Lott, T.R. Mager, R.P. Shogan, S.E. Yanichko, in: Radiation Embrittlement of Nuclear Reactor Pressure Vessel Steels, ASTM STP 909, ed. L.E. Steele (American Society for Testing and Materials, Philadelphia, PA, 1986) p. 242.
[37] J.R. Hawthorne, A.L. Hiser, Investigation of Irradiation-Anneal-Reirradiation (IAR) Properties Trends of RPV Welds, NUREG/CR-5492, MEA-2088, 1990.
[38] J.R. Hawthorne, Irradiation-Anneal-Reirradiation (IAR) Studies of Prototypic Reactor Vessel Weldments, NUREG/CR-5469, MEA-2364, 1989.
[39] S.A. Saltykov, Steriometric Metallography (Metallurgiya, Moscow, 1976).
[40] D. Briggs, M.P. Seah, eds., Practical Surface Analysis by Auger and X-ray Photoelectron Spectroscopy (Wiley, Chichester, 1983).
[41] H. Jones, M.G. Leak, Met. Sci. J. 1 (1967) 211.
[42] V. Misol, Interface Energy of Phases in Metals (Metallurgiya, Moscow, 1978).
[43] B.G. Livshits, V.S. Kraposhin, Ya.L. Linetskiy, Technical Properties of Metals and Alloys (Metallurgiya, Moscow, 1980).
[44] V.S. Zolotarevskiy, Mechanical Properties of Metals (Metallurgiya, Moscow, 1983).
[45] A.A. Popov, Strength Calculation Metods of Heating Elements of Nuclear Reactors (Energoatomizdat, Moscow, 1982).
[46] Yu.I. Likhachev, E.Ya. Pupko, Strength of Heating Elements of Nuclear Reactors (Atomizdat, Moscow, 1975).
[47] E.A. Kuleshova, E.V. Kolotukhin, E.E. Baryshev, G.V. Tyagunov, Metalloved. Term. Obrab. 6 (1995) 18.
[48] V.A. Nikolaev, Central Research Institute of Structural Materials 'Prometey', St.Peterburg, private communication.
[49] L.M. Utevski, E.E. Glicman, G.S. Kark, Reverse Temper Embrittlement of Steel and Iron Alloys (Metallurgiya, Moscow, 1985).
[50] L.M. Utevski, Temper Embrittlement of Steel (Metallurgizdat, Moscow, 1961).
[51] G.R. Odette, G.E. Lucas, in: Effects of Radiation on Materials, ASTM STP 1046, eds. N.H. Packan, R.E. Stoller and A.S. Kumar (American Society for Testing and Materials, Philadelphia, PA, 1990) p. 323.
[52] M.I. Goldshein, V.S. Litvinov, B.M. Bronfin, Material Science of High Strength Alloys (Metallurgiya, Moscow, 1986).
[53] V.A. Krokha, Curves of Material Hardening under Cold Deformation (Mashinostroenie, Moscow, 1968).
[54] K. Khertsberg, Deformation and Fracture Mechanics of Construction Materials (Metallurgiya, Moscow, 1989).
[55] G. Pusch, K.M. Petzold, H. Muhe, Neue Huette 22 (4) (1977) 223.
[56] L. Luyckx, J.R. Bell, A. McLean, M. Korchynsky, Metall. Trans. 1 (1970) 3341.
[57] U. Toaki, O. Rikuro, J. Iron Steel Inst. Jpn. 63 (11) (1977) 376.
[58] T. Imai, Y. Nishida, Nagoya Kogyo Gijutsu Shikensho Hokoku 34 (6) (1985) 159.
[59] T. Imai, Y. Nishida, Nagoya Kogyo Gijutsu Shikensho Hokoku 34 (6) (1985) 149.
[60] I.V. Gorynin, in: Metallovedenie (Sudpromgiz, Moscow, 1957) p. 145.
[61] I.V. Gorynin, in: Metallovedenie (Sudpromgiz, Moscow, 1957) p. 155.
[62] V.A. Bubnov, S.M. Kutepov, Himich. Neftyan. Mashinostroenie 4 (1989) 33.
[63] E. Fortner, L. Katz, N.L. Evanchan, Proc. 2nd Int. Conf. Mechanical Behaviour of Materials, Boston, MA, 1976, p. 1264.
[64] A.A. Astafiev, V.A. Yukhanov, A.D. Shur, Trudy TsNIITMASh 206 (1988) 7.
[65] J.-S. Wang, P.M. Anderson, Acta Metall. Mater. 39 (1991) 779.
[66] I.A. Vater, C.A. Hippsley, S.G. Druce, Int. J. Press. Vessel Piping 54 (1993) 31.
[67] Yu.I. Zvezdin, Yu.A. Nikolaev, D.M. Shur, Zavod. Lab. 2 (1993) 61.
[68] A.V. Nikolaeva, Yu.A. Nikolaev, A.M. Kryukov, J. Nucl. Mater. 211 (1994) 236.
[69] B.A. Gurovich, E.A. Kuleshova, O.V. Lavrenchuk, J. Nucl. Mater. 228 (1996) 330.
[70] A.V. Nikolaeva, Yu.A. Nikolaev, D.M. Shur, A.A. Chernobaeva, Fiz. Met. Metalloved. 76 (5) (1993) 163.
[71] M.P. Seah, Acta Metall. 25 (1977) 345.
[72] W.T. Tyson, Acta Metall. 26 (1978) 1471.
[73] M.K. Miller, R. Jayaram, P.J. Othen, G. Brauer, Appl. Surf. Sci. 76&77 (1994) 242.
[74] S.G. Druce, Acta Metall. 34 (1986) 219.
[75] J.A. Hudson, S.G. Druce, G. Gage, M. Wall, Theor. Appl. Fracture Mech. 10 (1988) 123.
[76] V.A. Nikolaev, V.V. Rybin, Vopr. Mater. 1 (1995) 41.
[77] Yu.A. Nikolaev, A.V. Nikolaeva, Mater. Sci. Forum 207–209 (1996) 653.
[78] T. Watanabe, H. Fujii, H. Oikawa, K.I. Arai, Acta Metall. 37 (1989) 941.
[79] M. Hashimoto, Y. Ishida, R. Yamamoto, M. Doyama, Acta Metall. 32 (1984) 1.
[80] J.T. Buswell, C.J. Bolton, M.R. Wootton, P.J.R. Bischler, R.B. Jones et al., in: Effects of Radiation on Materials, ASTM STP 1175, eds. A.S. Kumar, D.S. Gelles, R.K. Nanstad and E.A. Little (American Society for Testing and Materials, Philadelphia, PA, 1993) p. 332.
[81] A.D. Amaev, A.M. Kryukov, V.A. Nikolaev, P.A. Platonov et al., Radiation Stability of WWER Pressure Vessel Materials, Report of RMD of RRC 'Kurchatov Institute', No. 027915, Moscow, RRC 'KI', 1986.

[82] J.R. Hawthorne, Exploratory Studies of Element Interactions and Composition Dependencies in Radiation Sensetivity Development, NUREG/CR-4437, MEA-2113, 1985.
[83] F.A. Smidt, J.A. Sprague, Effects of Radiation on Substructure and Mechanical Properties of Metals and Alloys, ASTM STP 529 (American Society for Testing and Materials, Philadelphia, PA, 1973) p. 78.
[84] G.E. Lucas, G.R. Odette, R. Maiti, J.W. Sheckherd, in: Influence of Radiation on Material Properties, ASTM STP 956, eds. F.A. Garner, C.H. Henager and N. Igata (American Society for Testing and Materials, Philadelphia, PA, 1987) p. 379.
[85] K. Farrell, S.I. Mahmood, R.E. Stoller, L.K. Mansur, J. Nucl. Mater. 210 (1994) 268.
[86] R.K. Nanstad, R.G. Bergren, in: Effects of Radiation on Materials, ASTM STP 1175, eds. A.S. Kumar, D.S. Gelles, R.K. Nanstad and E.A. Little (American Society for Testing and Materials, Philadelphia, PA, 1993) p. 239.
[87] M. Brumovsky, A.M. Kryukov, F. Gillemo, V.I. Levit, Proc. IAEA Meeting, Vol. 2, Espoo, Finland, 1995.
[88] A.D. Amaev, A.M. Kryukov, M.A. Sokolov, in: Radiation Embrittlement of Nuclear Reactor Pressure Vessel Steels, ASTM STP 1170, ed. L.E. Steele (American Society for Testing and Materials, Philadelphia, PA, 1993) p. 369.
[89] W.L. Server, Effects of Radiation on Materials, ASTM STP 870 (American Society for Testing and Materials, Philadelphia, PA, 1985) p. 979.
[90] B. Macdonald, Effects of Radiation on Materials, ASTM STP 870 (American Society for Testing and Materials, Philadelphia, PA, 1985) p. 972.
[91] J.R. Hawthorne, NRL-8287, Naval Research Lab., 1979.
[92] T.R. Mager, EPRI NP-2712, Electric Power Research Inst., Vol. 2, 1982.
[93] J.R. Hawthorne, Exploratory Assessment of Post-Irradiaton Heat Treatment Variables in Notch Ductulity Recovery of A533B Steels, NUREG/CR-3229, MEA-2011, 1983.
[94] J.R. Hawthorne, NRL-8264, Naval Research Lab., 1979.
[95] J.R. Hawthorne, in: Influence of Radiation on Material Properties, ASTM STP 956, ed. F.A. Garner, C.H. Henager and N. Igata (American Society for Testing and Materials, Philadelphia, PA, 1987) p. 461.
[96] D. McLean, Grain Boundaries in Metals (Clarendon, Oxford, 1957).
[97] M. Große, J. Bömert, H.W. Viehrig, J. Nucl.Mater. 211 (1994) 177.
[98] P.M. Kelly, A. Jostsons, R.G. Blake, J.G. Napier, Phys. Status Solidi (a)31 (1975) 771.
[99] L.S. Davydova, M.V. Degtyariov, V.I. Levit, N.A. Smirnova, Fiz. Met. Metalloved. 61 (5) (1986) 963.
[100] K. Popp et al., in: Radiation Embrittlement of Nuclear Reactor Pressure Vessel Steels, ASTM STP 1170, ed. L.E. Steele (American Society for Testing and Materials, Philadelphia, PA, 1993) p. 344.
[101] P.R. Okamoto, L.E. Rehn, J. Nucl. Mater. 83 (1979) 2.
[102] A.A. Griffith, Philos. Trans. R. Soc. London 221A (1920) 163.
[103] N.N. Davidenkov, Problems of the Impact in Material Science (USSR Academy of Sciences, Moscow, 1938).
[104] N. Davidenkov, Dynamic Strength and Brittleness of Metalls, Vol. 1 (Naukova Dumka, Kiev, 1981).
[105] Yu.A. Nikolaev, Yu.N. Korolev, A.M. Kryukov, V.I. Levit, A.V. Nikolaeva et al., At. Energ. 80 (1) (1996) 33.
[106] A.V. Nikolaeva, Yu.A. Nikolaev, A.M. Kryukov, R.V. Arutyunyan, Fiz. Met. Metolloved. 77 (5) (1994) 171.
[107] P.A. Platonov, I.E. Tursunov, V.I. Levit, The Role of Radiation Enhanced Processes in Embrittlement of Steels, IAE-4478/11, Moscow, RRC'KI', 1987.